Supplementary materials

Supplementary Text

Figs. S1 to S19,

Table S1 to S8,

Data set 1

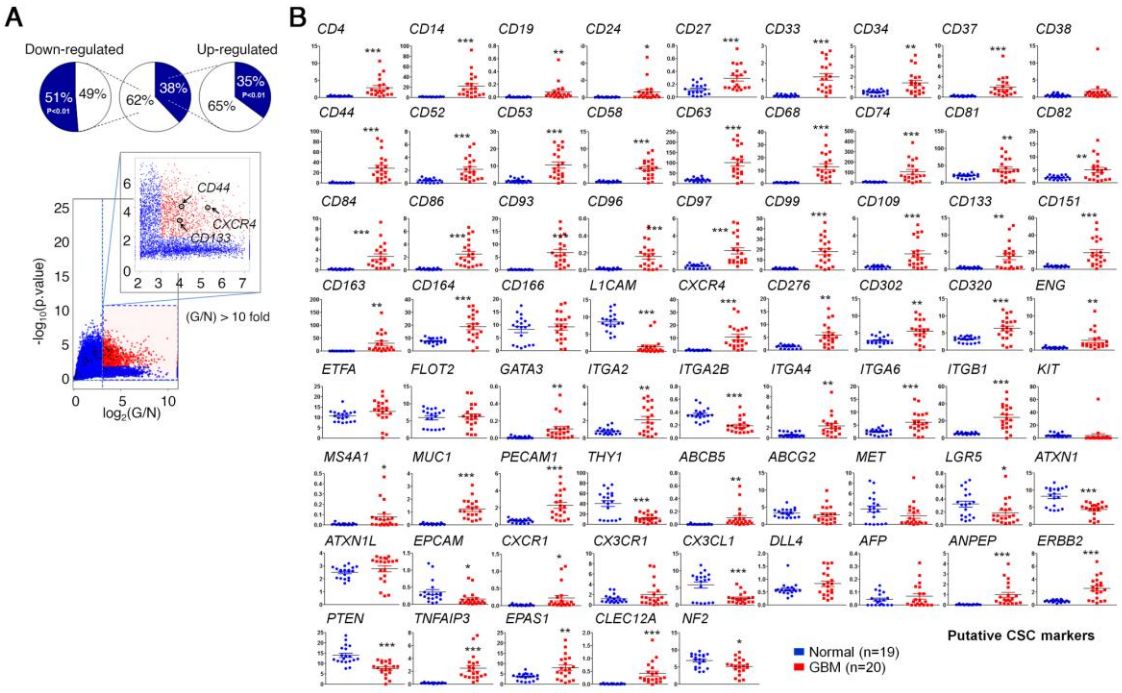

Fig. S1. Differential expression of known 69 tumor initiating genes in human normal brain and GBM tissue samples. (**A**) RNA sequencing analysis. (Upper) Venn diagram representing the number of transcripts (FPKM > 1) up- or down-regulated in human glioblastoma patient samples. (lower) Volcano plots displaying differentially

expressed genes. G/N, mean values derived from 20 human glioblastoma,G, samples divided by values from 19 human normal, N, brain tissues. In plot, red dots denote genes that undergo a statistically significant 10-fold change in G/N, either up or down ($P < 0.01$). Red-labeled dots have G/N ratios greater than 10-fold higher. Blue dot-labeled genes have G/N ratios between 2 to 10. (B) Data are shown as mean ± standard deviation for at least 19 independent specimens. Data are mean ± SD. *P* value by unpaired 2-tailed Student's *t* test

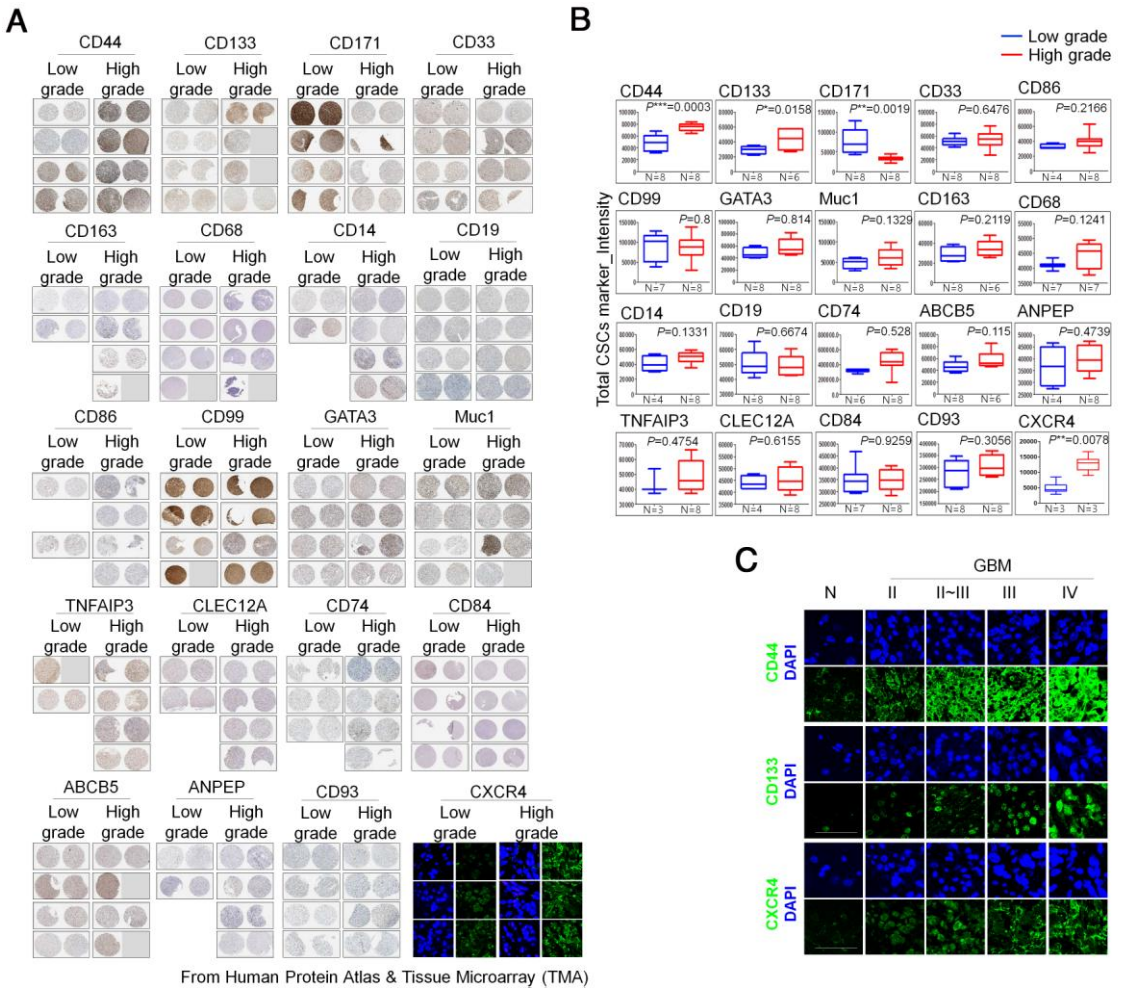

Fig. S2. High grade glioma exhibits high CD133 and CD44 markers expression.

(**A**) Low- and high- grade glioma tissue images stained with indicated antibodies were supported by the Human protein atlas (http://www.proteinatlas.org/) or obtained by staining of tissue microarray paraffin sections with CXCR4 antibody (last Panel). (**B**) Images in fig. S2A were quantified by Image J software. Data are mean ± SD (N>3). *P* value by unpaired 2-tailed Student's *t* test. (**C**) Tissue microarray paraffin sections from human glioblastoma tissues and normal brain tissues were subjected to immunofluorescent staining using antibodies against CXCR4, CD44, or CD133. Cells

were counter stained with DAPI. Images were captured using a Zeiss confocal microscope. Representative images were selected from at least three different fields.

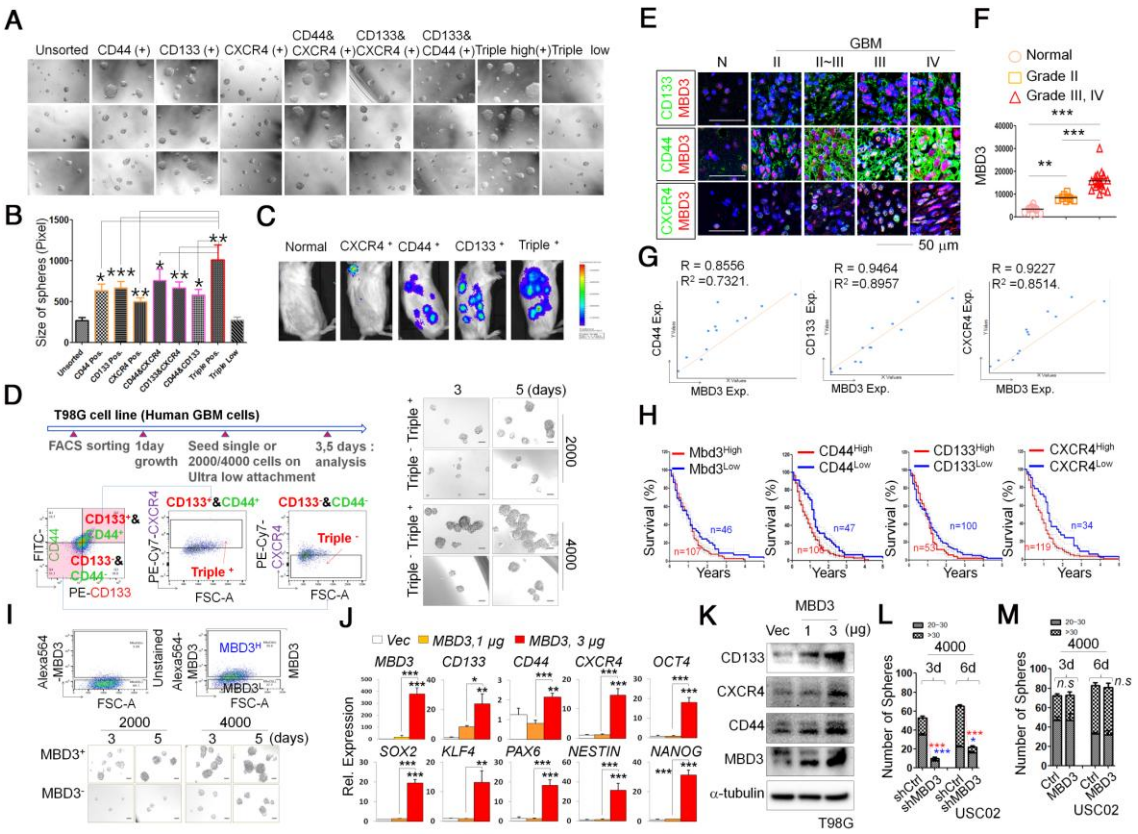

Fig. S3. Effect of MBD3 on self-renewal capacity of CD44, CD133, and CXCR4 triple high population. (**A**) CD44, CD133 and CXCR4 single, double, and triple- high or - low cells were sorted from dissociated sphere cells at a purity of 99.8% by FACS were seeded at a density of 5×10^3 cells/plate in ultra-low attachment 96-well plates for 5 days to allow sphere formation. (**B**) Relative sizes of SPs in fig. S3A were measured and quantified by Image J software. Data are mean ± SD (N>3). *P* value by One-way

ANOVA (Tukey's Multiple Comparison) test. (**C**) Cells from the indicated populations were injected into immunocompromised mice. After 1 weeks, bioluminescence imaging was used to monitor the initiation of tumor. (**D**) CD44, CD133 and CXCR4 triple positive or - negative cells were sorted from dissociated sphere cells at a purity of 99.8% by FACS were seeded as a density of 2×10^3 (N = 5) or 4×10^3 (N = 5) cells/well in ultra-low attachment 96-well plates for 1, 3 or 5 days to allow sphere formation. (**E** and **F**) Tissue microarray paraffin sections from human glioblastoma tissues (Stage II, N=8; II~III, N=8; III, N=8 and IV, N=8) and normal brain tissues (*n*=8) were subjected to immunefluorescent staining using antibodies against MBD3, CXCR4, CD44, or CD133. Cells were counter stained with DAPI. Images were captured using a Zeiss confocal microscope. Representative images were selected from at least three different fields. (**G**) Pearson correlation coefficient calculation of between Mbd3 and CSC markers expression from fig. S3E. (**H**) Kaplan–Meier plots showing survival rate by each transcripts expression level including *MBD3*, *CD44*, *CD133*, and *CXCR4* in GBM tumors of 153 patients from the Human Pathology Atlas (https://www.proteinatlas.org/). (**I**) MBD3 high or - low cells were sorted from T98G cells at a purity of 99.8% by FACS were seeded at single cell and a density of 2×10^3 (N = 5) or 4×10^3 (N = 5) cells/plate in ultra-low attachment 96-well plates for 1, 3 or 5

days to allow sphere formation. (Right) Representative images of SPs. Images were visualized using Zeiss fluorescence microscopy. Scale bar = 25 μm. (**J**, **K**) T98G cells were electroporated with 1 or 3 μg pUltra-Mbd3-Myc, and pUltra-control vectors using Amaxa Nucleofector and were grown on ultra-low attachment 96-well plates for up to 6 days. whole cell lysate was prepared for RT-qPCR (Fig. 3J) or immunoblotting (Fig. 3K). Data are mean ± SD (N=3 or 4). P value by One-way ANOVA (Tukey's Multiple Comparison) test. (**L**, **M**) USC02 GSCs infected by pUltra-Mbd3-Myc, pUltra-control, sh-scramble or shMBD3 lentivirus were seeded on ultra-low attachment 96-well plates and measured sphere sizes at the 3 or 6 days. Data are mean ± SD (N>3). P value by One-way ANOVA (Tukey's Multiple Comparison) test.

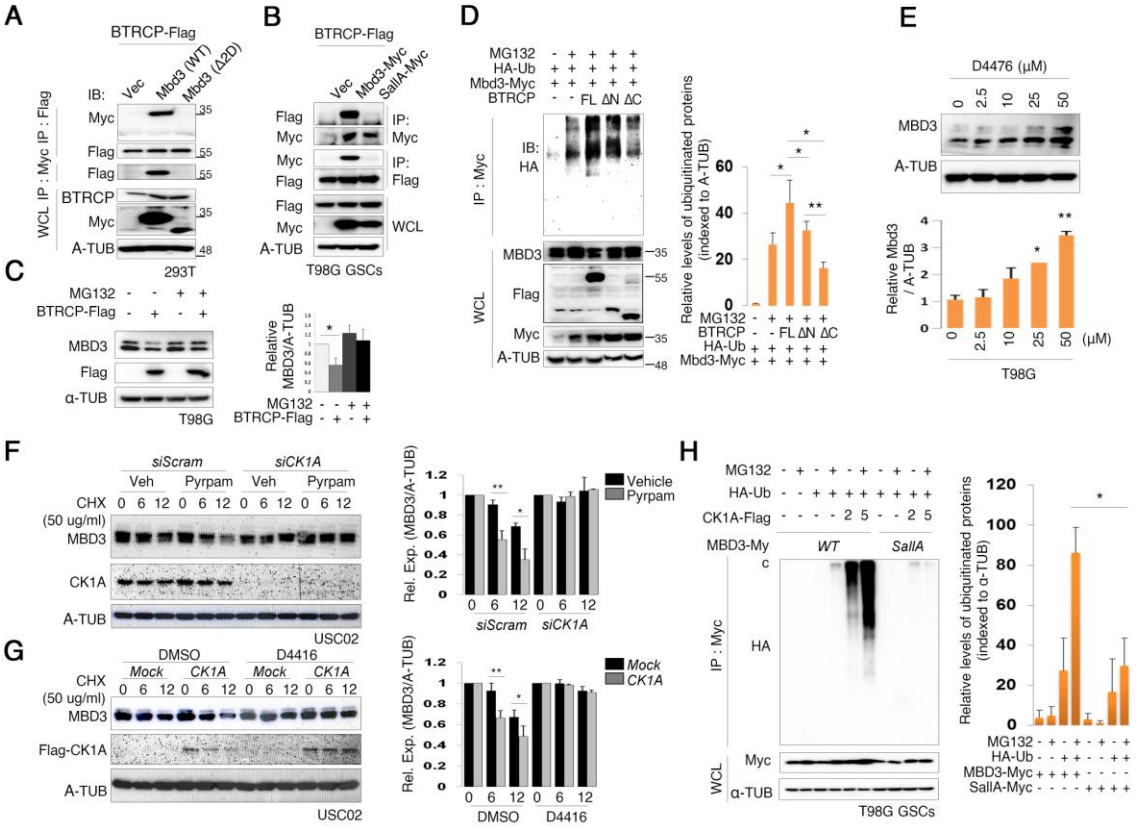

Fig. S4. β-TrCP is E3 ubiquitin ligase for Mbd3 polyubiquitination and proteasomal degradation. (**A**) Immunoprecipitation (IP) using Flag or Myc conjugated beads from lysates with β-TrCP-Flag plus control vector, wild-type Mbd3-Myc or mutant Mbd3 (Δ2D)-Myc. WCLs were subjected to immunoblotting using indicated antibodies. (**B**) IP using Myc- or Flag-conjugated beads from lysates transfected with β-TrCP-Flag plus control vector, wild type Mbd3-myc or mutant Mbd3 (S39,45,85,106A)-Myc. WCLs were subjected to immunoblotting using indicated antibodies. (**C**) (Upper) IB analysis of Mbd3, Flag and α-tubulin in lysates of HEK293 cells transfected with an empty or Flag-tagged β-TrCP vector and treated with or without MG132. (Lower)

Quantification of band intensity in (upper panel) using Image J software. (**D**) Quantification of Fig. 2N. Data are mean ± SD (N=3). *P* value by One-way ANOVA (Tukey's Multiple Comparison) test. (**E**) Lysates of T98G GSCs transfected with Flag-tagged full-length or mutant β-TrCP vectors with Mbd3-Myc vector were immunoprecipitated with indicated beads recognizing Myc. WCLs were immunoblotted (IB) with indicated antibodies. (Right) Quantification of polyubiquitylated Mbd3 normalized to α-tubulin. Data are mean ± SD (N=3). *P* value by One-way ANOVA (Tukey's Multiple Comparison) test. (**F**) (upper) Representative IB showing that the CK1α inhibitor D4476 increases Mbd3 protein abundance in a dose-dependent manner. (lower) Quantification of upper panel blots. Data are mean ± SD (N=3). *P* value by One-way ANOVA (Tukey's Multiple Comparison) test. (**G**) Effect of CK1α activation on Mbd3 polyubiquitylation. T98G GSCs were transfected with indicated vectors and WCLs were then immunoprecipitated with indicated beads recognizing Myc. Data are mean ± SD (N=3). *P* value by One-way ANOVA (Tukey's Multiple Comparison) test. (**H**) T98G GSCs were transfected with wild type Mbd3-Myc or mutant (S39,45,85,106A, SallA)-Myc and HA-Ub expression vectors plus increasing levels of Flag-tagged CK1α vector and treated one day later with MG132 for 6 hours before harvest. After lysis, IP was performed with Flag-M2 beads. WCLs were analyzed by IB

with indicated antibodies. (**I**) USC02 GSCs were transfected with control or CK1α shRNA and treated with DMSO or pyrpam (2 μM) and cycloheximide (CHX) for indicated times (h=hours) before harvest. WCLs were immunoblotted (IB) with indicated antibodies. (right) Quantification of MBD3 normalized to α-tubulin. Data are mean ± SD (N=3). *P* value by One-way ANOVA (Tukey's Multiple Comparison) test. (**J**) USC02 GSCs were transfected with pcDNA3.1-Empty or pcDNA3.1-CK1α and treated with DMSO or CK1α inhibitor, D4416 (10 μM) and cycloheximide (CHX) for indicated times (h=hours) before harvest. WCLs were immunoblotted (IB) with indicated antibodies. (right) Data are mean ± SD (N=3). *P* value by One-way ANOVA (Tukey's Multiple Comparison) test.

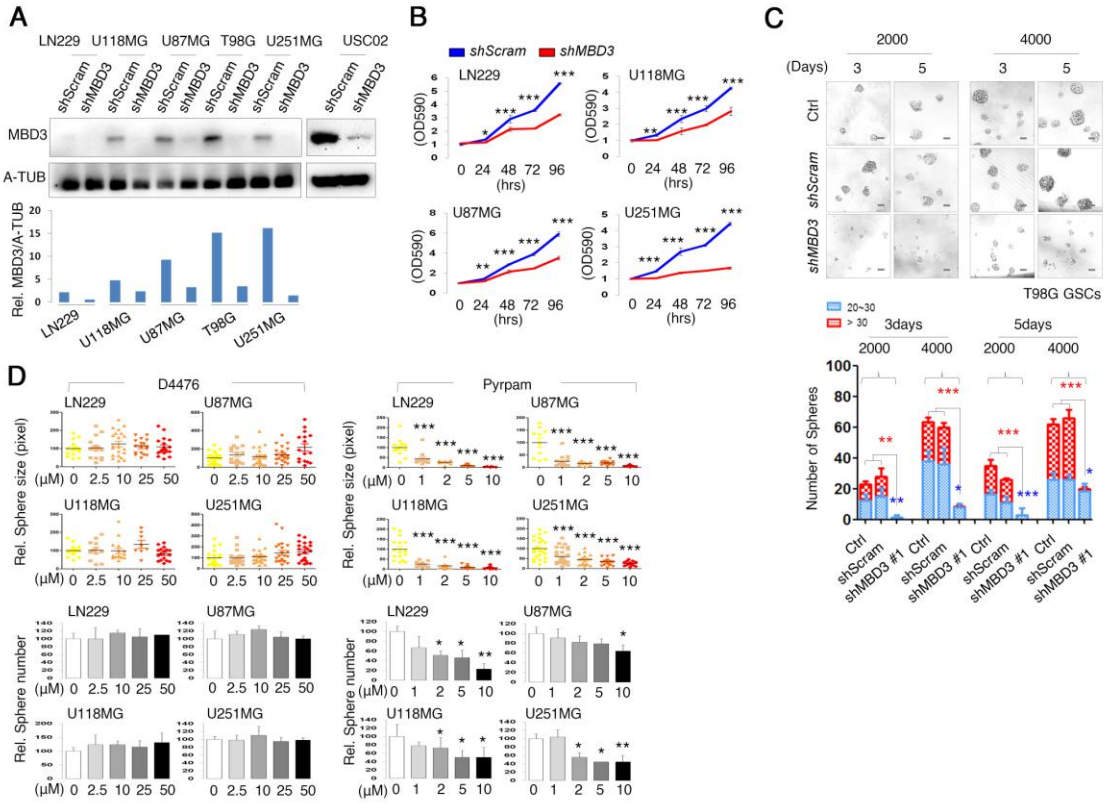

Fig. S5. Effect of Mbd3 knockdown in proliferation and self-renewal activity of GBM cells. (**A**) GBM cell lines were infected by pLKO3G-shMbd3 #1 and #2 lentiviral vectors and shcontrol or shMbd3 knockdown stable GBM cells were subjected to immunoblotting analysis with indicated antibodies. (Lower) Mbd3 levels in (A, upper) were normalized to α-tubulin. (**B** and **C**) GBM cells infected by sh-scramble or shMbd3 lentivirus were seeded on 6-well plates and assayed for colony formation. Foci were photographed (B) and quantified (C). Data are mean ± SD (N=3). *P* value by One-way ANOVA (Tukey's Multiple Comparison) test. (**D**) Proliferation of shcontrol or shMbd3 knockdown stable GBM cells were quantified using an MTT assay. Data are mean ± SD

(N>3). *P* value by One-way ANOVA (Tukey's Multiple Comparison) test. (**E**, upper) Naïve, shcontrol or shMbd3 knockdown T98G-GSCs were seeded at a density of 2 × 10^3 (N = 5) or 4 × 10^3 (N = 5) cells/plate in ultra-low attachment 96-well plates for 1, 3 or 5 days to allow sphere formation. (**E**, lower) Relative sizes and number of spheres shown in upper panels were quantified using Image J software. Data are mean ± SD (N>3). *P* value by One-way ANOVA (Tukey's Multiple Comparison) test. (**F** and **G**) GBM cells were seeded at a density of 2 × 10^4 cells/plate in ultra-low attachment 96-well plates and then treated with indicated concentration of D4476 or Pyrpam for 3 days to allow sphere formation. Relative size or number of spheres of each group were measured by Image J software. Data are mean ± SD (N>8). *P* value by One-way ANOVA (Tukey's Multiple Comparison) test.

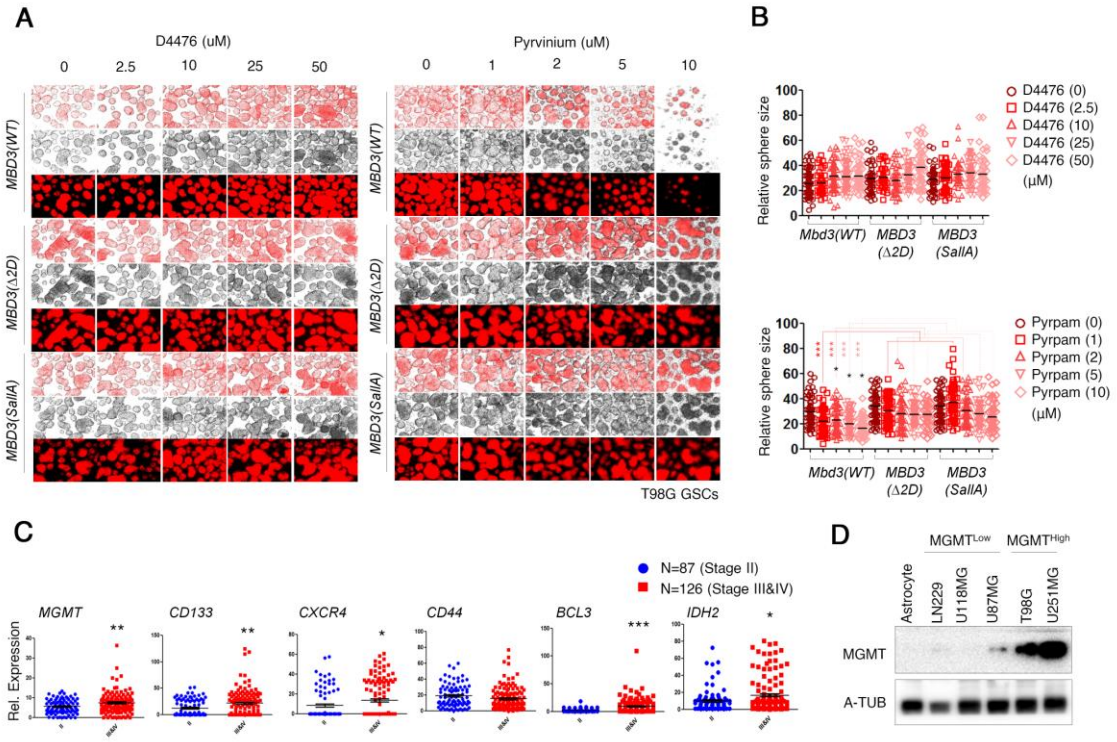

Fig. S6. Effect of Pyrvinum pamoate in proliferation and self-renewal activity of GBM cells. (**A** and **B**) (upper) T98G GSCs depleted by shMbd3 were infected by Wild-type (WT) Mbd3 or mutant forms (Δ2D and S39/45/85/106A labeled as SallA)-mcherry lentivirus and then Mbd3 (WT), (Δ2D), and (SallA) T98G GSCs expressing mCherry were sorted by FACS. Each cell was seeded at a density of 2×10^4 cells/plate in ultra-low attachment 96-well plates and then treated with indicated concentration of D4476 or Pyrpam for 3 days to allow sphere formation. (Lower) Relative size of SP of each group were measured by Image J software. Data are mean ± SD (N>3). *P* value by One-way ANOVA (Tukey's Multiple Comparison) test. (**C**) Analysis of RNA sequencing data set which are consist of 272 patients' samples containing different stages of gliomas (stage

II, N = 87; stage III, N = 47; stage IV, N = 79). Data are mean ± SD. *P* value by One way ANOVA (Tukey's Multiple Comparison) test. (**D**) Immunoblotting analysis with indicated antibodies.

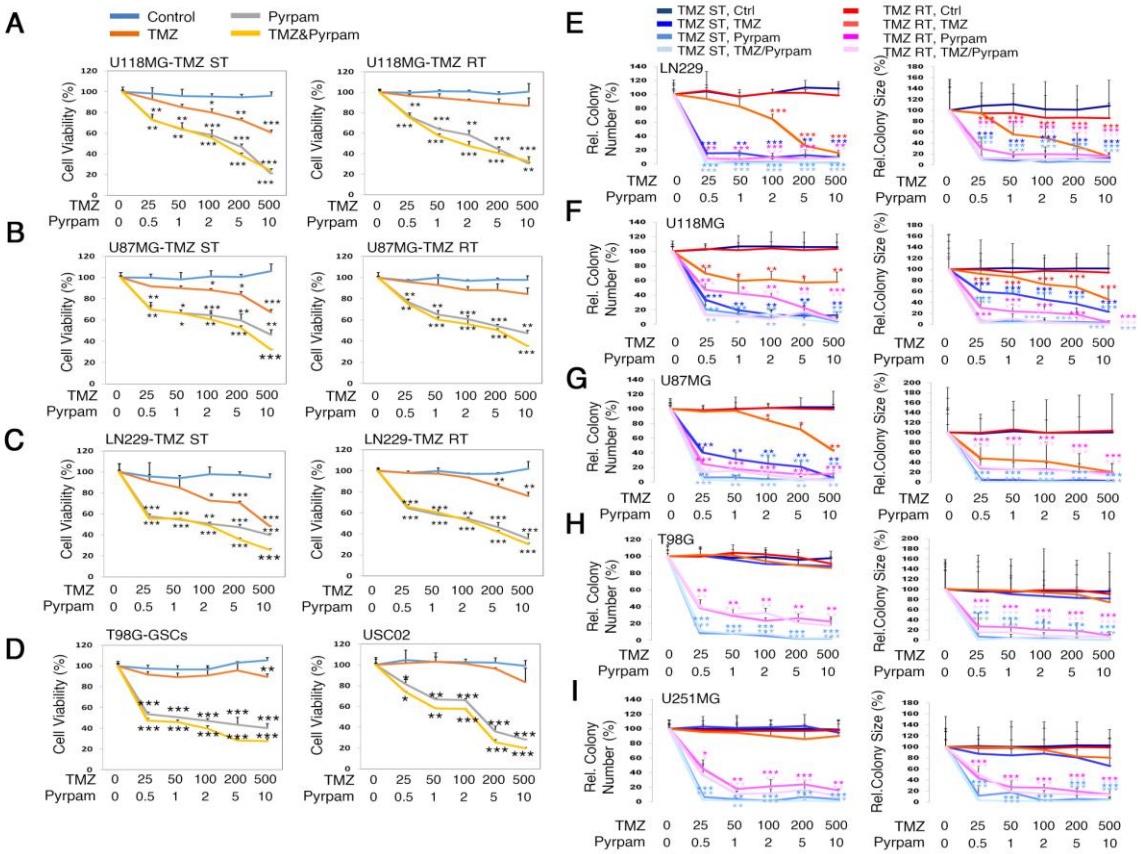

Fig. S7. Effects of Pyrpam on temozolomide (TMZ)-sensitive and -resistant GBM cells. (**A-D**) TMZ-sensitive (ST) and –resistant (RT) GBM or GSCs were treated with varying dose of TMZ, Pyrpam or their combination for 48 hours, and proliferation was quantified using a MTT assay. Data are mean ± SD (N>3). *P* value by One-way ANOVA (Tukey's Multiple Comparison) test. (**E-I**) TMZ ST- or RT GBM or GSCs

were seeded on 6-well plates and assayed for colony formation. Drug were treated with varying dose of TMZ, Pyrpam or their combination for 48 hours, and then cultured for another 10 to 12 days in fresh medium. The number or size of colony was quantified using image J software. Data are mean ± SD (N=3). *P* value by One-way ANOVA (Tukey's Multiple Comparison) test.

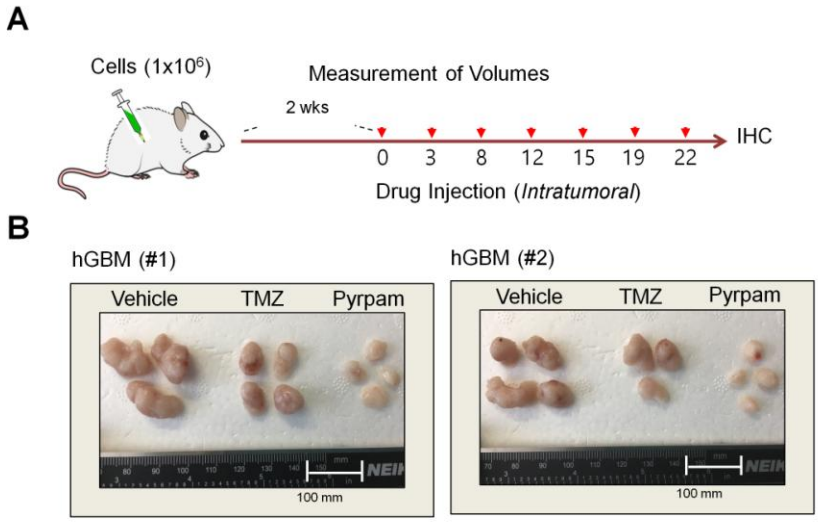

Fig. S8. Mbd3 Loss or destabilization by CK1α-β-TrCP-Mbd3 signaling activation inhibits progression of TMZ-resistant GSCs or GBM with high MGMT expression. (**A** and **B**) Qualitative results of Fig. 5, E and G. Images were captured using a Zeiss confocal microscope. Representative images were selected from at least 3 different fields. (**C**) (upper) Schematic showing injection of GBM cells in Fig. 5L experiment. Human primary GBM cells (1×10^6) in 200 μL phosphate-buffered saline/Matrigel (1:1) were subcutaneously (s.c.) injected into the dorsal flank of immunocompromised mice

mice (N=3 or 4 per group). (Lower) Images of tumors isolated from immunocompromised mice injected with two different human primary GBM cells. Scale bar = 100 mm.

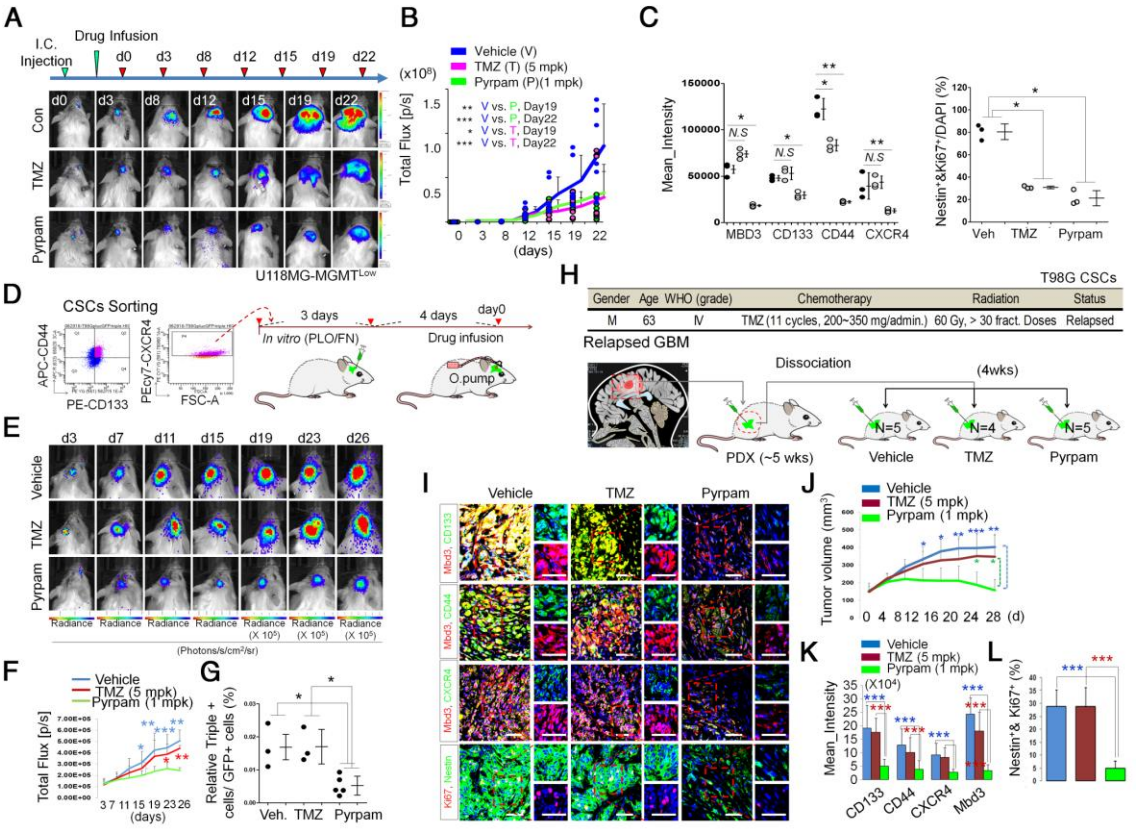

Fig. S9. Effect of Pyrpam in GBM Progression and Recurrence Following Temozolomide (TMZ) and Radiation Treatment. (**A**, upper) Schematic showing injection of GBM cells and intrathecal infusion of drugs (vehicle, TMZ (5 mg/kg per day), Pyrpam (1 mg/kg per day)) for 22 days using implanted osmotic pump. pLuc-U118MG cells were intracranially injected into immuno-compromised (NSG) mice (N

= 4 or 5 per group). (**A**, lower) Representative bioluminescence images of mice at indicated times after intracranial injection. (**B**) Tumor volume was measured every 3 or 4 days. Quantification (total flux, photons per second=p/s) of the bioluminescent signal from tumor regions in **A**. Data are mean ± SD (n= 4 or 5). *P* value by Two-way ANOVA (Bonferroni posttests) test. (**C**) After 4 weeks, mice were sacrificed and analyzed immunohistochemically with indicated antibodies. Expression of CD133, CD44, CXCR4, MBD3, Ki67, and Nestin was quantified using Image J software. Data are mean ± SD. *P* value by One-way ANOVA (Tukey's Multiple Comparison) test. (**D**) Schematic showing injection of sorted GSCs and intrathecal infusion of drugs (vehicle, TMZ (5 mg/kg per day), Pyrpam (1 mg/kg per day)) for 26 days using implanted osmotic pump. (**E**) Representative bioluminescence images of mice at indicated times after intracranial injection. (**F**) Tumor volume was measured every 3 or 4 days. Quantification (total flux, photons per second=p/s) of the bioluminescent signal from tumor regions in **E**. Data are mean ± SD (n= 5 or 6). *P* value by Two-way ANOVA (Bonferroni posttests) test. (**G**) FACS analysis of CD44/CD133/CXCR4 triple-positive populations within GBMs in xenografted tumors derived from various GSCs. (**H**) Schematic showing patient information (upper), and subcutaneous (s.c.) injection of dissociated human tumors into immunocompromised mice plus intra-tumoral injection

of vehicle, TMZ (5 mg/kg per day), and Pyrpam (1 mg/kg per day) (lower, n=4 or 5). (**I**) Tumor volume was measured every 4 days. Data are mean ± SD (n=4 or 5). *P* value by Two-way ANOVA (Bonferroni posttests) test. (**J**) After 4 weeks, mice were sacrificed and analyzed immunohistochemically with indicated antibodies. (**K** and **L**) Expression of CD44, CD133, CXCR4, Mbd3 in **K**, Ki67, and Nestin in **L** in a GBM in each representative xenograft GBM tumor in **J** was quantified using Image J software. Images were captured using a Zeiss confocal microscope. Representative images were selected from at least 3 different fields. Data are mean ± SD (N>3). *P* value by One-way ANOVA (Tukey's Multiple Comparison) test.

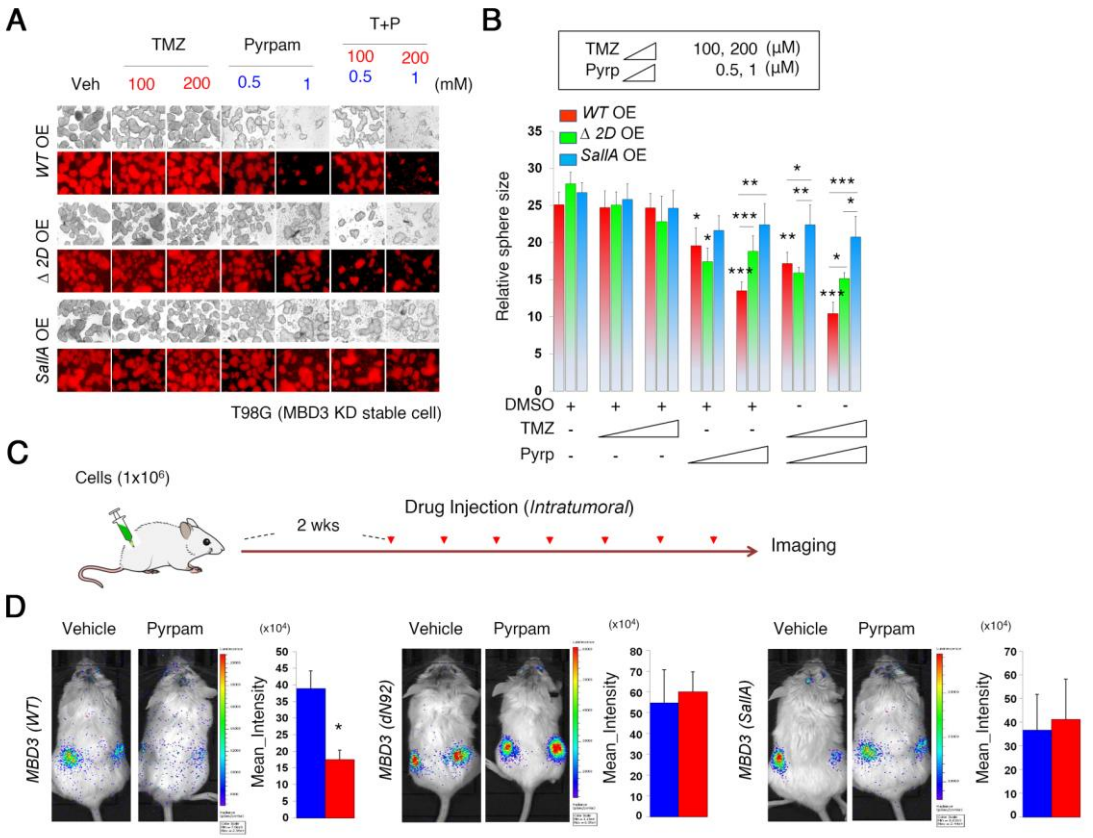

Fig. S10. Pyrpam inhibits progression of GBM cells expressing wild-Type Mbd3, but not those expressing phospho-defective mutants of Mbd3. (**A** and **B**) Wild-type Mbd3 (WT) or its mutant forms (Δ2D), and (SallA) T98G cells expressing mCherry were seeded on 12 well plates and treated with indicated concentrations of TMZ, Pyrpam, or both for 8 days. Sphere forming assays were performed. Spheres were photographed and (right) quantified using Image J software. Data are mean ± SD (N>3). *P* value by One-way ANOVA (Tukey's Multiple Comparison) test. (**C** and **D**) Schematic showing in vivo xenograft experiment, and subcutaneous (s.c.) injection of Wild-type MBD3 (WT) or its mutant forms (Δ2D), and (SallA) T98G cells into

immunocompromised mice plus intratumoral injection of vehicle, TMZ (5 mg/kg per day), and Pyrpam (1 mg/kg per day) (lower, n = 4). (**D**) Quantification (total flux, photons per second=p/s) of the bioluminescent signal from tumor regions**.** (**P* < 0.05). Data are mean ± SD (n=3). *P* value by unpaired 2-tailed Student's *t* test.

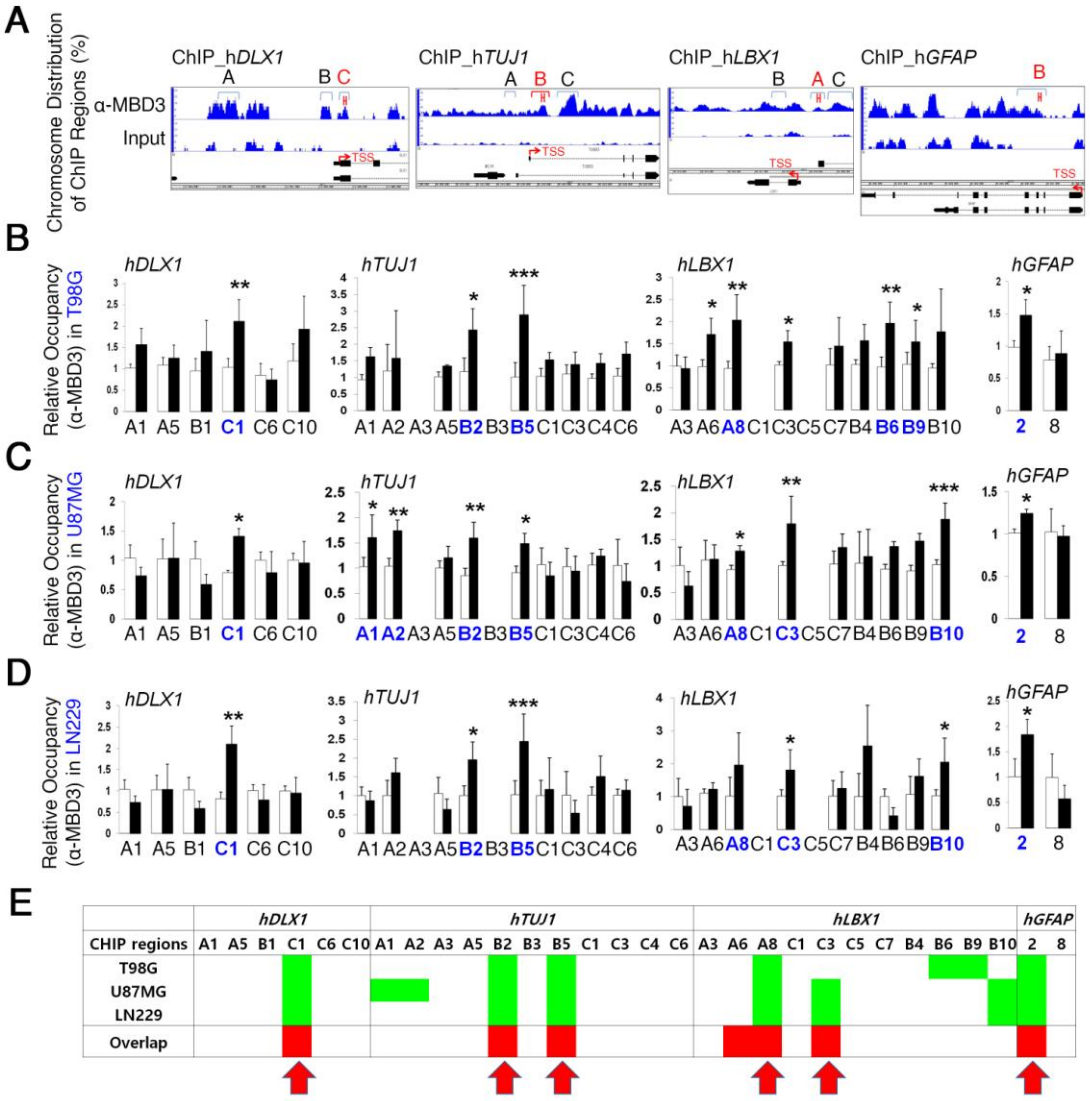

Fig. S11. MBD3 and nucleosomal remodeling histone deacetylase (NuRD) complex components colocalize on neural differentiation associated gene promoters and gene bodies. (**A**) Human MBD3-chromatin immunoprecipitation sequencing (ChIP-seq) analysis in Breast Cancer Cells (GSE44737)[1]. MBD3-binding peaks in Breast Cancer Cells in differentiation genes such as *Dlx1*, *Tuj1*, *Lbx1*, and *Gfap*. (**B**-**D**) ChIP-qPCR analysis of MBD3 occupancy at the putative MBD3-binding loci of T98G in fig. S11B, U87MG in Fig. S11C, and LN229 in fig. S11D of GBM cell lines. (**E**) ChIP-qPCR analysis of MBD3 identify gene loci that overlap in three different GBM cell lines. Red arrows indicate overlapped gene loci obtained from the MBD3 ChIP-qPCR analysis using three different GBM cell lines. All values in fig S11, B to D correspond to the mean ± SD (N>3). *P* value by Two-way ANOVA (Bonferroni posttests) test.

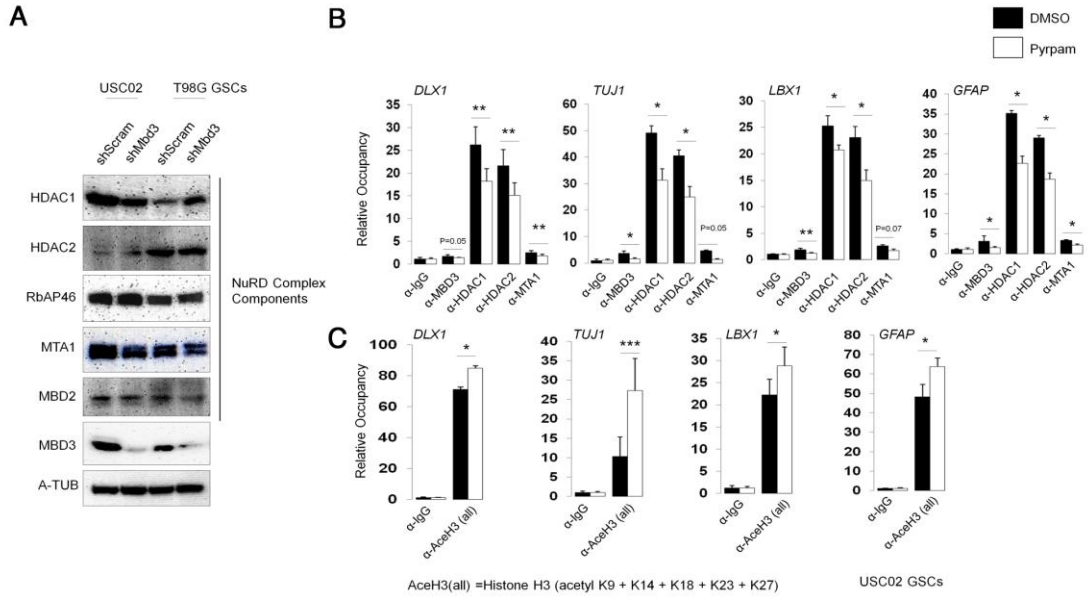

Fig. S12. MBD3 loss doesn't change protein expression of NuRD complex components and decreases occupancy of MBD3-NuRD complex components on neural differentiation associated gene promoters and gene bodies in GSCs. (**A**) USC02 or T98G GSCs were infected by pLKO3G-shMBD3 #1 and #2 lentiviral vectors and shcontrol or shMBD3 knockdown GSC cells were subjected to immunoblotting analysis with indicated antibodies. (**B** and **C**) ChIP-qPCR analysis of MBD3, HDAC1, HDAC2, MTA1, and acetyl histone H3 occupancy at MBD3-binding locus in USC02 GSCs treated with DMSO (N = 3) and Pyrvinium pamoate (N = 3). Immunoglobulin G (IgG) ChIP served as a negative control. Values are normalized to input control and represent mean ± SD (N=3). *P* value by One-way ANOVA (Tukey's Multiple Comparison) test.

REFERENCES

1. Shimbo, T., *et al.* MBD3 localizes at promoters, gene bodies and enhancers of active genes. *PLoS genetics* 9, e1004028 (2013).

Supplemental Tables

Supplementary Table S1. Clinicopathological features of 39 subjects with RNA sequencing.

No.	Patients	Site	Sex	Age	Race	RIN
1	RL15	CEREBELLUM	F	55	C	7.1
2	RL16	CEREBELLUM	F	56	C	7.8
3	RL17	CEREBELLUM	F	57	C	5.6
4	RL18	CEREBELLUM	M	55	C	6.3
5	RL19	CEREBELLUM	M	55	C	6
6	RL20	CEREBELLUM	M	57	C	6.3
7	RL21	CORTEX	F	60	C	7.7
8	RL22	CORTEX	M	60	C	8.1
9	RL23	CORTEX	F	60	C	7.1
10	RL24	CORTEX	M	56	C	6
11	RL25	CORTEX	F	56	C	7.4
12	RL26	CORTEX	M	56	C	6.1
13	RL40	CORTEX	M	64	C	7.3
14	RL41	CORTEX	M	62	C	4.2
15	RL42	CORTEX	M	56	A	7.4
16	RL43	CORTEX	F	82	C	6.9
17	RL44	CORTEX	F	61	C	6.8
18	RL45	CORTEX	M	55	C	5.4
19	RL46	CORTEX	F	63	C	6.8
20	RL1	GBM	M	63	C	7.1
21	RL2	GBM	F	43	C	7
22	RL3	GBM	F	57	C	3.8
23	RL4	GBM	M	58	C	1.1
24	RL5	GBM	M	56	C	2.8
25	RL6	GBM	M	57	C	2.2
26	RL7	GBM	F	43	C	7.9
27	RL27	GBM	M	81	C	6.9
28	RL28	GBM	F	59	C	8

29	RL29	GBM	F	57	C	8.3
30	RL30	GBM	M	39	C	7.5
31	RL31	GBM	F	50	C	7.8
32	RL32	GBM	M	49	C	7.3
33	RL33	GBM	F	76	A	7
34	RL34	GBM	M	64	C	2.3
35	RL35	GBM	M	48	C	6.5
36	RL36	GBM	M	54	A	6
37	RL37	GBM	M	61	C	7.4
38	RL38	GBM	M	76	C	7.5
39	RL39	GBM	M	66	C	8.1
GBM = glioblastoma multiforme; **Cortex** = cortical brain controls; **Cerebellum**: cerebellar controls.,**C** = Caucasian; **A** = Asian; **H** = Hispanic, **RIN** = RNA integrity number						

Supplementary Table S2. 69 putative cell surface cancer stem cell or progenitor markers analyzed with RNA sequencing

No	**Gene**	**No**	**Gene**	**No**	**Gene**	**No**	**Gene**
1	CD4	**19**	CD84 (SLAMF5)	**37**	ETFA	**55**	ATXN1L
2	CD14	**20**	CD86	**38**	FLOT2	**56**	EPCAM
3	CD19	**21**	CD93	**39**	GATA3	**57**	CXCR1
4	CD24	**22**	CD96	**40**	ITGA2	**58**	CX3CR1
5	CD27	**23**	CD97	**41**	ITGA2B	**59**	CX3CL1
6	CD33	**24**	CD99	**42**	ITGA4	**60**	DLL4
7	CD34	**25**	CD109	**43**	ITGA6	**61**	AFP
8	CD37	**26**	CD133	**44**	ITGB1	**62**	ANPEP (=CD13)
9	CD38	**27**	CD151	**45**	KIT (=CD117)	**63**	ERBB2
10	CD44	**28**	CD163	**46**	MS4A1	**64**	PTEN

					(=CD20)		
11	CD52	**29**	CD164	**47**	MUC1	**65**	TNFAIP3 (=A20)
12	CD53	**30**	CD166	**48**	PECAM1	**66**	EPAS1
13	CD58	**31**	CD171	**49**	THY1(=CD90)	**67**	CLEC12A
14	CD63	**32**	CD184	**50**	ABCB5	**68**	THY1
15	CD68	**33**	CD276	**51**	ABCG2	**69**	NF2
16	CD74	**34**	CD302	**52**	MET		
17	CD81	**35**	CD320	**53**	LGR5		
18	CD82	**36**	ENG (Endoglin/CD105)	**54**	ATXN1		

Type of Cancer	**(Cancer) Stem Cell Markers (Reference)**
Glioma/Medulloblastoma	EPAS1 (=HIF2A) (1), TNFAIP3 (=A20) (2), CD171 (=L1CAM) (3), CX3CR1 (4), CX3CL1 (4)
Glioblastoma	CD109 (5), ITGA6 (6), CD44 (7), CD133 (7), CD97 (8)
Thyroid Cancer	PECAM1 (9), ITGA4 (9), CD34 (9), CD38 (9)
Head&Neck Cancer	CD44 (10), ABCG2 (11), CD133 (12), CD44 (12), MET (13), CD168 (14)
Lung Cancer	KIT (15), THY1 (16), ABCG2 (17), EPCAM (17), CD74 (18), CD164 (19), ETFA (20)
Breast Cancer	CD14 (21), CD24 (22), CD29 (23), CD133 (24), CD44 (25), CD81 (26), CD184 (27), FLOT2 (28), ITGA6 (29), CXCR1 (30), ErbB2 (31), PTEN (32), ATXN1 (33), CD276 (B7-H3) (34), ITGB1 (35), Muc1 (36), CD81 (26)
Gastric Cancer	CXCR4 (CD181), CD44 (37), CD163 (38), CD133 (39), Lgr5 (39)
Liver Cancer	KIT (40), CD34 (40), CD24 (40), THY1 (=CD90) (40), AFP (40), EPCAM (40), CD133 (40), CD44 (40), AFP (41), EPCAM (41), ANPEP (=CD13) (40), NF2 (42)
Pancreatic Cancer	CD44 (43), MUC1 (44)
Colon Cancer	CD44 (45), CD133 (45), CD58 (46), CD166 (45), Lgr5 (47), EPCAM (48), DLL4 (49)
Prostate Cancer	CD44 (37), CD81 (26), CD151 (50), ABCG2 (51), CD68

	(52)
Kidney Cancer	ENG (Endoglin/CD105) (53)
Osteosarcoma	CD44 (54), CD133 (54)
Ovarian Cancer	CD24 (55), CD44 (55), CD133 (55), CD117 (=c-KIT) (55), ENG (Endoglin/CD105) (56), GATA3 (57)
Leukemia	CD33 (58), CD37 (59), CD52 (60), CD82 (61), CD96 (62), KIT (63), CLEC12A (64), CD93 (65), CD302 (66)
Lymphoma	CD320 (67) (68)
Myeloma	CD19 (69), CD27 (69), CD38 (69), MS4A1 (70), ABCB5 (69), CD99 (71)
Melanoma	CD133 (72), MS4A1 (=CD20) (72), ABCB5 (73), ABCG2 (74)
Hematopoietic Stem Cell	CD53 (75), CD63 (75), ATxN1L (76), CD84 (SLAMF5) (77), CD164 (78), ITGA2B (79), CD86 (78)
Stem-like Immune Cell	CD4 (80)

References

1. Li Z, Bao S, Wu Q, Wang H, Eyler C, Sathornsumetee S, et al. Hypoxia-inducible factors regulate tumorigenic capacity of glioma stem cells. *Cancer cell.* 2009;15(6):501-13.
2. Hjelmeland AB, Wu Q, Wickman S, Eyler C, Heddleston J, Shi Q, et al. Targeting A20 decreases glioma stem cell survival and tumor growth. *PLoS biology.* 2010;8(2):e1000319.
3. Bao S, Wu Q, Li Z, Sathornsumetee S, Wang H, McLendon RE, et al. Targeting cancer stem cells through L1CAM suppresses glioma growth. *Cancer research.* 2008;68(15):6043-8.
4. Erreni M, Solinas G, Brescia P, Osti D, Zunino F, Colombo P, et al. Human glioblastoma tumours and neural cancer stem cells express the chemokine CX3CL1 and its receptor CX3CR1. *Eur J Cancer.* 2010;46(18):3383-92.
5. Minata M, Audia A, Shi J, Lu S, Bernstock J, Pavlyukov MS, et al. Phenotypic Plasticity of Invasive Edge Glioma Stem-like Cells in Response to Ionizing Radiation. *Cell reports.* 2019;26(7):1893-905 e7.
6. Lathia JD, Gallagher J, Heddleston JM, Wang J, Eyler CE, Macswords J, et al. Integrin alpha 6 regulates glioblastoma stem cells. *Cell stem cell.* 2010;6(5):421-32.

7. Brown DV, Filiz G, Daniel PM, Hollande F, Dworkin S, Amiridis S, et al. Expression of CD133 and CD44 in glioblastoma stem cells correlates with cell proliferation, phenotype stability and intra-tumor heterogeneity. *PloS one.* 2017;12(2):e0172791.
8. Safaee M, Fakurnejad S, Bloch O, Clark AJ, Ivan ME, Sun MZ, et al. Proportional upregulation of CD97 isoforms in glioblastoma and glioblastoma-derived brain tumor initiating cells. *PloS one.* 2015;10(2):e0111532.
9. Liotti F, Collina F, Pone E, La Sala L, Franco R, Prevete N, et al. Interleukin-8, but not the Related Chemokine CXCL1, Sustains an Autocrine Circuit Necessary for the Properties and Functions of Thyroid Cancer Stem Cells. *Stem Cells.* 2017;35(1):135-46.
10. Trapasso S, and Allegra E. Role of CD44 as a marker of cancer stem cells in head and neck cancer. *Biologics : targets & therapy.* 2012;6:379-83.
11. Shen B, Dong P, Li D, and Gao S. Expression and function of ABCG2 in head and neck squamous cell carcinoma and cell lines. *Experimental and therapeutic medicine.* 2011;2(6):1151-7.
12. Satpute PS, Hazarey V, Ahmed R, and Yadav L. Cancer stem cells in head and neck squamous cell carcinoma: a review. *Asian Pacific journal of cancer prevention : APJCP.* 2013;14(10):5579-87.
13. Xiao M, Liu L, Zhang S, Yang X, and Wang Y. Cancer stem cell biomarkers for head and neck squamous cell carcinoma: A bioinformatic analysis. *Oncology reports.* 2018;40(6):3843-51.
14. Johrens K, Anagnostopoulos I, Dommerich S, Raguse JD, Szczepek AJ, Klauschen F, et al. Expression patterns of CD168 correlate with the stage and grade of squamous cell carcinoma of head and neck. *Molecular and clinical oncology.* 2017;6(4):597-602.
15. Levina V, Marrangoni A, Wang T, Parikh S, Su Y, Herberman R, et al. Elimination of human lung cancer stem cells through targeting of the stem cell factor-c-kit autocrine signaling loop. *Cancer research.* 2010;70(1):338-46.
16. Herreros-Pomares A, de-Maya-Girones JD, Calabuig-Farinas S, Lucas R, Martinez A, Pardo-Sanchez JM, et al. Lung tumorspheres reveal cancer stem cell-like properties and a score with prognostic impact in resected non-small-cell lung cancer. *Cell death & disease.* 2019;10(9):660.
17. Zakaria N, Satar NA, Abu Halim NH, Ngalim SH, Yusoff NM, Lin J, et al. Targeting Lung Cancer Stem Cells: Research and Clinical Impacts. *Frontiers in oncology.* 2017;7:80.

18. Murayama T, Nakaoku T, Enari M, Nishimura T, Tominaga K, Nakata A, et al. Oncogenic Fusion Gene CD74-NRG1 Confers Cancer Stem Cell-like Properties in Lung Cancer through a IGF2 Autocrine/Paracrine Circuit. *Cancer research.* 2016;76(4):974-83.
19. Chen WL, Huang AF, Huang SM, Ho CL, Chang YL, and Chan JY. CD164 promotes lung tumor-initiating cells with stem cell activity and determines tumor growth and drug resistance via Akt/mTOR signaling. *Oncotarget.* 2017;8(33):54115-35.
20. Bonuccelli G, Peiris-Pages M, Ozsvari B, Martinez-Outschoorn UE, Sotgia F, and Lisanti MP. Targeting cancer stem cell propagation with palbociclib, a CDK4/6 inhibitor: Telomerase drives tumor cell heterogeneity. *Oncotarget.* 2017;8(6):9868-84.
21. Hwang-Verslues WW, Kuo WH, Chang PH, Pan CC, Wang HH, Tsai ST, et al. Multiple lineages of human breast cancer stem/progenitor cells identified by profiling with stem cell markers. *PloS one.* 2009;4(12):e8377.
22. Rostoker R, Abelson S, Genkin I, Ben-Shmuel S, Sachidanandam R, Scheinman EJ, et al. CD24(+) cells fuel rapid tumor growth and display high metastatic capacity. *Breast cancer research : BCR.* 2015;17:78.
23. Vassilopoulos A, Chisholm C, Lahusen T, Zheng H, and Deng CX. A critical role of CD29 and CD49f in mediating metastasis for cancer-initiating cells isolated from a Brca1-associated mouse model of breast cancer. *Oncogene.* 2014;33(47):5477-82.
24. Cordone I, Masi S, Summa V, Carosi M, Vidiri A, Fabi A, et al. Overexpression of syndecan-1, MUC-1, and putative stem cell markers in breast cancer leptomeningeal metastasis: a cerebrospinal fluid flow cytometry study. *Breast cancer research : BCR.* 2017;19(1):46.
25. Al-Hajj M, Wicha MS, Benito-Hernandez A, Morrison SJ, and Clarke MF. Prospective identification of tumorigenic breast cancer cells. *Proceedings of the National Academy of Sciences of the United States of America.* 2003;100(7):3983-8.
26. Kumar D, Gupta D, Shankar S, and Srivastava RK. Biomolecular characterization of exosomes released from cancer stem cells: Possible implications for biomarker and treatment of cancer. *Oncotarget.* 2015;6(5):3280-91.
27. Trautmann F, Cojoc M, Kurth I, Melin N, Bouchez LC, Dubrovska A, et al. CXCR4 as biomarker for radioresistant cancer stem cells. *International journal*

of radiation biology. 2014;90(8):687-99.

28. Velapasamy S, Dawson CW, Young LS, Paterson IC, and Yap LF. The Dynamic Roles of TGF-beta Signalling in EBV-Associated Cancers. *Cancers.* 2018;10(8).
29. Cariati M, Naderi A, Brown JP, Smalley MJ, Pinder SE, Caldas C, et al. Alpha-6 integrin is necessary for the tumourigenicity of a stem cell-like subpopulation within the MCF7 breast cancer cell line. *International journal of cancer.* 2008;122(2):298-304.
30. Brandolini L, Cristiano L, Fidoamore A, De Pizzol M, Di Giacomo E, Florio TM, et al. Targeting CXCR1 on breast cancer stem cells: signaling pathways and clinical application modelling. *Oncotarget.* 2015;6(41):43375-94.
31. Wang X, Sun Y, Wong J, and Conklin DS. PPARgamma maintains ERBB2-positive breast cancer stem cells. *Oncogene.* 2013;32(49):5512-21.
32. Korkaya H, Paulson A, Charafe-Jauffret E, Ginestier C, Brown M, Dutcher J, et al. Regulation of mammary stem/progenitor cells by PTEN/Akt/beta-catenin signaling. *PLoS biology.* 2009;7(6):e1000121.
33. Ke J, Zhao Z, Hong SH, Bai S, He Z, Malik F, et al. Role of microRNA221 in regulating normal mammary epithelial hierarchy and breast cancer stem-like cells. *Oncotarget.* 2015;6(6):3709-21.
34. Liu Z, Zhang W, Phillips JB, Arora R, McClellan S, Li J, et al. Immunoregulatory protein B7-H3 regulates cancer stem cell enrichment and drug resistance through MVP-mediated MEK activation. *Oncogene.* 2019;38(1):88-102.
35. Barnawi R, Al-Khaldi S, Colak D, Tulbah A, Al-Tweigeri T, Fallatah M, et al. beta1 Integrin is essential for fascin-mediated breast cancer stem cell function and disease progression. *International journal of cancer.* 2019;145(3):830-41.
36. Alam M, Rajabi H, Ahmad R, Jin C, and Kufe D. Targeting the MUC1-C oncoprotein inhibits self-renewal capacity of breast cancer cells. *Oncotarget.* 2014;5(9):2622-34.
37. Collins AT, Berry PA, Hyde C, Stower MJ, and Maitland NJ. Prospective identification of tumorigenic prostate cancer stem cells. *Cancer research.* 2005;65(23):10946-51.
38. Cheng Z, Zhang D, Gong B, Wang P, and Liu F. CD163 as a novel target gene of STAT3 is a potential therapeutic target for gastric cancer. *Oncotarget.* 2017;8(50):87244-62.
39. Singh SR. Gastric cancer stem cells: a novel therapeutic target. *Cancer letters.* 2013;338(1):110-9.

40. Xiao Y, Lin M, Jiang X, Ye J, Guo T, Shi Y, et al. The Recent Advances on Liver Cancer Stem Cells: Biomarkers, Separation, and Therapy. *Anal Cell Pathol (Amst).* 2017;2017:5108653.
41. Sun JH, Luo Q, Liu LL, and Song GB. Liver cancer stem cell markers: Progression and therapeutic implications. *World journal of gastroenterology.* 2016;22(13):3547-57.
42. Benhamouche S, Curto M, Saotome I, Gladden AB, Liu CH, Giovannini M, et al. Nf2/Merlin controls progenitor homeostasis and tumorigenesis in the liver. *Genes & development.* 2010;24(16):1718-30.
43. Li C, Heidt DG, Dalerba P, Burant CF, Zhang L, Adsay V, et al. Identification of pancreatic cancer stem cells. *Cancer research.* 2007;67(3):1030-7.
44. Curry JM, Thompson KJ, Rao SG, Besmer DM, Murphy AM, Grdzelishvili VZ, et al. The use of a novel MUC1 antibody to identify cancer stem cells and circulating MUC1 in mice and patients with pancreatic cancer. *Journal of surgical oncology.* 2013;107(7):713-22.
45. Moon BS, Jeong WJ, Park J, Kim TI, Min do S, and Choi KY. Role of oncogenic K-Ras in cancer stem cell activation by aberrant Wnt/beta-catenin signaling. *Journal of the National Cancer Institute.* 2014;106(2):djt373.
46. Xu S, Wen Z, Jiang Q, Zhu L, Feng S, Zhao Y, et al. CD58, a novel surface marker, promotes self-renewal of tumor-initiating cells in colorectal cancer. *Oncogene.* 2015;34(12):1520-31.
47. Morgan RG, Mortensson E, and Williams AC. Targeting LGR5 in Colorectal Cancer: therapeutic gold or too plastic? *British journal of cancer.* 2018;118(11):1410-8.
48. Gires O, Klein CA, and Baeuerle PA. On the abundance of EpCAM on cancer stem cells. *Nature reviews Cancer.* 2009;9(2):143; author reply
49. Badenes M, Trindade A, Pissarra H, Lopes-da-Costa L, and Duarte A. Delta-like 4/Notch signaling promotes Apc (Min/+) tumor initiation through angiogenic and non-angiogenic related mechanisms. *BMC cancer.* 2017;17(1):50.
50. Williamson SC, Hepburn AC, Wilson L, Coffey K, Ryan-Munden CA, Pal D, et al. Human alpha(2)beta(1)(HI) CD133(+VE) epithelial prostate stem cells express low levels of active androgen receptor. *PloS one.* 2012;7(11):e48944.
51. Westover D, and Li F. New trends for overcoming ABCG2/BCRP-mediated resistance to cancer therapies. *Journal of experimental & clinical cancer research : CR.* 2015;34:159.
52. Huang H, Wang C, Liu F, Li HZ, Peng G, Gao X, et al. Reciprocal Network

between Cancer Stem-Like Cells and Macrophages Facilitates the Progression and Androgen Deprivation Therapy Resistance of Prostate Cancer. *Clinical cancer research : an official journal of the American Association for Cancer Research.* 2018;24(18):4612-26.

53. Hu J, Guan W, Yan L, Ye Z, Wu L, and Xu H. Cancer Stem Cell Marker Endoglin (CD105) Induces Epithelial Mesenchymal Transition (EMT) but Not Metastasis in Clear Cell Renal Cell Carcinoma. *Stem cells international.* 2019;2019:9060152.
54. Zhao D, Wang S, Chu X, and Han D. LncRNA HIF2PUT inhibited osteosarcoma stem cells proliferation, migration and invasion by regulating HIF2 expression. *Artificial cells, nanomedicine, and biotechnology.* 2019;47(1):1342-8.
55. Klemba A, Purzycka-Olewiecka JK, Wcislo G, Czarnecka AM, Lewicki S, Lesyng B, et al. Surface markers of cancer stem-like cells of ovarian cancer and their clinical relevance. *Contemp Oncol (Pozn).* 2018;22(1A):48-55.
56. Zhang J, Yuan B, Zhang H, and Li H. Human epithelial ovarian cancer cells expressing CD105, CD44 and CD106 surface markers exhibit increased invasive capacity and drug resistance. *Oncology letters.* 2019;17(6):5351-60.
57. Chen HJ, Huang RL, Liew PL, Su PH, Chen LY, Weng YC, et al. GATA3 as a master regulator and therapeutic target in ovarian high-grade serous carcinoma stem cells. *International journal of cancer.* 2018;143(12):3106-19.
58. Walter RB, Appelbaum FR, Estey EH, and Bernstein ID. Acute myeloid leukemia stem cells and CD33-targeted immunotherapy. *Blood.* 2012;119(26):6198-208.
59. De Kouchkovsky I, and Abdul-Hay M. 'Acute myeloid leukemia: a comprehensive review and 2016 update'. *Blood cancer journal.* 2016;6(7):e441.
60. Blatt K, Herrmann H, Hoermann G, Willmann M, Cerny-Reiterer S, Sadovnik I, et al. Identification of campath-1 (CD52) as novel drug target in neoplastic stem cells in 5q-patients with MDS and AML. *Clinical cancer research : an official journal of the American Association for Cancer Research.* 2014;20(13):3589-602.
61. Nishioka C, Ikezoe T, Furihata M, Yang J, Serada S, Naka T, et al. CD34(+)/CD38(-) acute myelogenous leukemia cells aberrantly express CD82 which regulates adhesion and survival of leukemia stem cells. *International journal of cancer.* 2013;132(9):2006-19.
62. Hosen N, Park CY, Tatsumi N, Oji Y, Sugiyama H, Gramatzki M, et al. CD96 is

a leukemic stem cell-specific marker in human acute myeloid leukemia. *Proceedings of the National Academy of Sciences of the United States of America.* 2007;104(26):11008-13.

63. Somervaille TC, and Cleary ML. Identification and characterization of leukemia stem cells in murine MLL-AF9 acute myeloid leukemia. *Cancer cell.* 2006;10(4):257-68.
64. Morsink LM, Walter RB, and Ossenkoppele GJ. Prognostic and therapeutic role of CLEC12A in acute myeloid leukemia. *Blood reviews.* 2019;34:26-33.
65. Iwasaki M, Liedtke M, Gentles AJ, and Cleary ML. CD93 Marks a Non-Quiescent Human Leukemia Stem Cell Population and Is Required for Development of MLL-Rearranged Acute Myeloid Leukemia. *Cell stem cell.* 2015;17(4):412-21.
66. Lo TH, Abadir E, Gasiorowski RE, Kabani K, Ramesh M, Orellana D, et al. Examination of CD302 as a potential therapeutic target for acute myeloid leukemia. *PloS one.* 2019;14(5):e0216368.
67. Li L, Yoon SO, Fu DD, Zhang X, and Choi YS. Novel follicular dendritic cell molecule, 8D6, collaborates with CD44 in supporting lymphomagenesis by a Burkitt lymphoma cell line, L3055. *Blood.* 2004;104(3):815-21.
68. Margolin DA, Myers T, Zhang X, Bertoni DM, Reuter BA, Obokhare I, et al. The critical roles of tumor-initiating cells and the lymph node stromal microenvironment in human colorectal cancer extranodal metastasis using a unique humanized orthotopic mouse model. *FASEB journal : official publication of the Federation of American Societies for Experimental Biology.* 2015;29(8):3571-81.
69. Hajek R, Okubote SA, and Svachova H. Myeloma stem cell concepts, heterogeneity and plasticity of multiple myeloma. *British journal of haematology.* 2013;163(5):551-64.
70. Johnsen HE, Bogsted M, Schmitz A, Bodker JS, El-Galaly TC, Johansen P, et al. The myeloma stem cell concept, revisited: from phenomenology to operational terms. *Haematologica.* 2016;101(12):1451-9.
71. Chung SS, Eng WS, Hu W, Khalaj M, Garrett-Bakelman FE, Tavakkoli M, et al. CD99 is a therapeutic target on disease stem cells in myeloid malignancies. *Science translational medicine.* 2017;9(374).
72. Fang D, Nguyen TK, Leishear K, Finko R, Kulp AN, Hotz S, et al. A tumorigenic subpopulation with stem cell properties in melanomas. *Cancer research.* 2005;65(20):9328-37.

73. Schatton T, Murphy GF, Frank NY, Yamaura K, Waaga-Gasser AM, Gasser M, et al. Identification of cells initiating human melanomas. *Nature.* 2008;451(7176):345-9.
74. Marzagalli M, Moretti RM, Messi E, Marelli MM, Fontana F, Anastasia A, et al. Targeting melanoma stem cells with the Vitamin E derivative delta-tocotrienol. *Scientific reports.* 2018;8(1):587.
75. Beckmann J, Scheitza S, Wernet P, Fischer JC, and Giebel B. Asymmetric cell division within the human hematopoietic stem and progenitor cell compartment: identification of asymmetrically segregating proteins. *Blood.* 2007;109(12):5494-501.
76. Kahle JJ, Souroullas GP, Yu P, Zohren F, Lee Y, Shaw CA, et al. Ataxin1L is a regulator of HSC function highlighting the utility of cross-tissue comparisons for gene discovery. *PLoS genetics.* 2013;9(3):e1003359.
77. Sintes J, Romero X, de Salort J, Terhorst C, and Engel P. Mouse CD84 is a pan-leukocyte cell-surface molecule that modulates LPS-induced cytokine secretion by macrophages. *Journal of leukocyte biology.* 2010;88(4):687-97.
78. Shimazu T, Iida R, Zhang Q, Welner RS, Medina KL, Alberola-Lla J, et al. CD86 is expressed on murine hematopoietic stem cells and denotes lymphopoietic potential. *Blood.* 2012;119(21):4889-97.
79. Dumon S, Walton DS, Volpe G, Wilson N, Dasse E, Del Pozzo W, et al. Itga2b regulation at the onset of definitive hematopoiesis and commitment to differentiation. *PloS one.* 2012;7(8):e43300.
80. Hong H, Gu Y, Sheng SY, Lu CG, Zou JY, and Wu CY. The Distribution of Human Stem Cell-like Memory T Cell in Lung Cancer. *J Immunother.* 2016;39(6):233-40.

Supplementary Table S3. 153 human patient information used for TCGA Analyses

Sample	Description	Sample	Description
TCGA-12-3650-01A	46 years, male, white	TCGA-32-2615-01A	62 years, male, white
TCGA-19-1390-01A	63 years, female, white	TCGA-12-5295-01A	60 years, female, white
TCGA-19-2629-01A	60 years, male, white	TCGA-28-5216-01A	52 years, male, white
TCGA-06-0744-01A	67 years, male, white	TCGA-12-0619-01A	60 years, male, white
TCGA-06-0743-01A	69 years, male, white	TCGA-76-4929-01A	76 years, female, white
TCGA-06-0747-01A	53 years, male, white	TCGA-06-2557-01A	76 years, male, black or african american

TCGA-27-2523-01A	63 years, male, white	TCGA-27-1830-01A	57 years, male, white
TCGA-14-1034-01A	60 years, female	TCGA-28-1747-01C	44 years, male, white
TCGA-26-5134-01A	74 years, male, white	TCGA-14-2554-01A	52 years, female, white
TCGA-26-5135-01A	72 years, female, white	TCGA-06-0649-01B	73 years, female, black or african american
TCGA-06-0686-01A	53 years, male, white	TCGA-06-5416-01A	23 years, female, white
TCGA-15-0742-01A	65 years, male, white	TCGA-14-0817-01A	69 years, female, white
TCGA-32-1970-01A	59 years, male, white	TCGA-06-2558-01A	75 years, female, white
TCGA-19-2625-01A	76 years, female, white	TCGA-19-2619-01A	55 years, female, black or african american
TCGA-28-1753-01A	53 years, male, white	TCGA-76-4926-01B	68 years, male, white
TCGA-41-5651-01A	59 years, female, black or african american	TCGA-06-5856-01A	58 years, male, white
TCGA-02-2483-01A	43 years, male, asian	TCGA-06-2561-01A	53 years, female, white
TCGA-76-4927-01A	58 years, male, white	TCGA-06-5859-01A	63 years, male, white
TCGA-06-2570-01A	21 years, female, white	TCGA-28-5220-01A	67 years, male, white
TCGA-27-2521-01A	34 years, male, white	TCGA-06-0644-01A	71 years, male, black or african american
TCGA-41-2572-01A	67 years, male, white	TCGA-06-0882-01A	30 years, male, white
TCGA-26-5132-01A	74 years, male, white	TCGA-06-0878-01A	74 years, male, white
TCGA-27-2524-01A	56 years, male, white	TCGA-41-4097-01A	63 years, female, white
TCGA-06-0125-01A	63 years, female, white	TCGA-15-1444-01A	21 years, male, white
TCGA-14-0787-01A	69 years, male, asian	TCGA-28-5204-01A	72 years, male, white
TCGA-02-2485-01A	53 years, male, black or african american	TCGA-06-0238-01A	46 years, male, white
TCGA-28-5209-01A	66 years, female, white	TCGA-06-0184-01A	63 years, male, white
TCGA-06-0745-01A	59 years, male, white	TCGA-06-0130-01A	54 years, male, white
TCGA-41-2571-01A	89 years, male, white	TCGA-06-0187-01A	69 years, male, white
TCGA-06-0211-01B	47 years, male, white	TCGA-27-1834-01A	56 years, male, white
TCGA-06-0157-01A	63 years, female, white	TCGA-12-5299-01A	56 years, female, white
TCGA-26-5139-01A	65 years, female, white	TCGA-06-2564-01A	50 years, male, white
TCGA-06-0174-01A	54 years, male, white	TCGA-28-5218-01A	63 years, male, white
TCGA-06-0158-01A	73 years, male, white	TCGA-14-0781-01B	49 years, male, black or african american
TCGA-19-2624-01A	51 years, male, white	TCGA-06-5413-01A	67 years, male, white

TCGA-32-2616-01A	48 years, female, white	TCGA-76-4928-01B	85 years, female, white
TCGA-32-2634-01A	82 years, male, white	TCGA-02-2486-01A	64 years, male, white
TCGA-26-5133-01A	59 years, male, white	TCGA-06-2562-01A	81 years, male, white
TCGA-14-0790-01B	64 years, female, white	TCGA-06-5418-01A	75 years, female, white
TCGA-12-3652-01A	60 years, male, white	TCGA-06-0138-01A	43 years, male, white
TCGA-27-2519-01A	48 years, male, white	TCGA-26-5136-01B	78 years, female, white
TCGA-14-1825-01A	70 years, male, white	TCGA-14-0871-01A	75 years, female, white
TCGA-08-0386-01A	74 years, male, white	TCGA-28-2499-01A	59 years, male, white
TCGA-12-3653-01A	34 years, female, white	TCGA-06-2569-01A	24 years, female, black or african american
TCGA-16-0846-01A	85 years, male, white	TCGA-06-0210-01A	72 years, female, white
TCGA-28-2513-01A	69 years, female, white	TCGA-06-5412-01A	78 years, female, white
TCGA-06-0156-01A	57 years, male, white	TCGA-06-2559-01A	83 years, male, white
TCGA-76-4931-01A	70 years, female, white	TCGA-02-0047-01A	78 years, male, white
TCGA-06-0129-01A	30 years, male, asian	TCGA-19-1787-01B	49 years, male, white
TCGA-06-5408-01A	54 years, female, white	TCGA-16-1045-01B	49 years, female, white
TCGA-32-2638-01A	67 years, male, white	TCGA-06-5411-01A	51 years, male, white
TCGA-12-0616-01A	36 years, female, white	TCGA-06-5410-01A	72 years, female, white
TCGA-06-0749-01A	50 years, male, black or african american	TCGA-28-5207-01A	71 years, male, white
TCGA-27-1837-01A	36 years, male, white	TCGA-32-1980-01A	72 years, male, white
TCGA-06-1804-01A	81 years, female, white	TCGA-26-1442-01A	43 years, male, white
TCGA-41-3915-01A	48 years, male, white	TCGA-02-0055-01A	62 years, female, white
TCGA-76-4925-01A	76 years, male, white	TCGA-19-4065-01A	36 years, male, white
TCGA-06-5414-01A	61 years, male, white	TCGA-06-0141-01A	62 years, male, white
TCGA-27-2528-01A	62 years, male, white	TCGA-06-5417-01A	45 years, female, white
TCGA-06-0190-01A	62 years, male, white	TCGA-27-2526-01A	79 years, female, white
TCGA-06-2563-01A	72 years, female, white	TCGA-06-0132-01A	49 years, male, white
TCGA-28-5208-01A	52 years, male, white	TCGA-06-0139-01A	40 years, male, white
TCGA-06-0750-01A	43 years, male, white	TCGA-28-5213-01A	72 years, male, white
TCGA-12-0821-01A	62 years, male, white	TCGA-32-5222-01A	66 years, male, white
TCGA-28-2514-01A	45 years, male, asian	TCGA-06-0178-01A	39 years, male, white
TCGA-06-0168-01A	59 years, female, white	TCGA-06-0219-01A	67 years, male, white
TCGA-14-0789-01A	54 years, male, white	TCGA-14-1823-01A	58 years, female, white
TCGA-06-0646-01A	61 years, male, white	TCGA-14-1829-01A	57 years, male, black or

			african american
TCGA-06-2565-01A	59 years, male, asian	TCGA-28-2509-01A	77 years, female, white
TCGA-19-5960-01A	56 years, male, white	TCGA-27-1832-01A	59 years, female, white
TCGA-06-2567-01A	65 years, male, white	TCGA-32-2632-01A	80 years, male, white
TCGA-27-1835-01A	53 years, female, white	TCGA-12-0618-01A	49 years, male, white
TCGA-32-1982-01A	76 years, female, white	TCGA-06-5858-01A	45 years, female, white
TCGA-32-4213-01A	47 years, female, white	TCGA-06-0645-01A	56 years, female, white
TCGA-28-5215-01A	62 years, female, white	TCGA-12-1597-01B	62 years, female, white
TCGA-76-4932-01A	50 years, female, white	TCGA-19-2620-01A	70 years, male, white

Supplementary Table S4. The list of results obtained from the Mass spectrometry (MS) analysis of Flag-MBD3 in T98G cells.

Unique	Total	Reference	Gene Symbol	MWT(kDa)	AVG
5	5	P63208_SKP1_HUMAN	SKP1	18.65	3.668
3	3	Q13618_CUL3_HUMAN	CUL3	88.87	3.0207
3	3	Q13617_CUL2_HUMAN	CUL2	86.93	2.0008
2	2	Q13616_CUL1_HUMAN	CUL1	89.62	3.2357
1	1	Q9Y297_FBW1A_HUMAN	FBW1A	68.87	3.5635
1	1	P63208_SKP1_HUMAN	SKP1	18.65	3.5731
1	1	Q93034_CUL5_HUMAN	CUL5	90.9	3.5668
2	2	O75083_WDR1_HUMAN	WDR1	66.15	3.1045
1	2	Q9BZH6_WDR11_HUMAN	WDR11	136.6	4.1936
1	1	Q9GZL7_WDR12_HUMAN	WDR12	47.68	4.2976
1	2	Q9GZL7_WDR12_HUMAN	WDR12	47.68	3.7652
2	2	Q8NI36_WDR36_HUMAN	WDR36	105.26	4.6827
1	1	Q8NI36_WDR36_HUMAN	WDR36	105.26	2.5706
2	2	Q9GZS3_WDR61_HUMAN	WDR61	33.56	3.4202
3	4	Q9GZS3_WDR61_HUMAN	WDR61	33.56	3.2014
1	1	Q6RFH5_WDR74_HUMAN	WDR74	42.41	3.7702
5	6	Q9BQA1_MEP50_HUMAN	WDR77	36.7	3.9328
5	6	Q9BQA1_MEP50_HUMAN	WDR77	36.7	4.4334
1	1	Q6UXN9_WDR82_HUMAN	WDR82	35.06	3.5807

2	2	P16455_MGMT_HUMAN	MGMT	21.63	3.6122
3	3	P48735_IDHP_HUMAN	IDH2	50.88	3.1843
1	1	P26358_DNMT1_HUMAN	DNMT1	183.05	2.833
2	2	Q9UBB5_MBD2_HUMAN	MBD2	43.23	2.0073
17	32	O95983_MBD3_HUMAN	MBD3	32.82	3.436
10	10	Q12873_CHD3_HUMAN	CHD3	226.45	3.1775
4	5	Q12873_CHD3_HUMAN	CHD3	226.45	3.0176
35	43	Q14839_CHD4_HUMAN	CHD4	217.87	2.8225
8	8	Q13330_MTA1_HUMAN	MTA1	80.74	2.5918
21	22	O94776_MTA2_HUMAN	MTA2	74.98	2.9738
7	7	Q9BTC8_MTA3_HUMAN	MTA3	67.46	2.4561
18	42	Q13547_HDAC1_HUMAN	HDAC1	55.07	3.1017
15	31	Q92769_HDAC2_HUMAN	HDAC2	55.33	3.3458
2	3	O15379_HDAC3_HUMAN	HDAC3	48.82	1.9058
2	2	P01112_RASH_HUMAN	HRAS	21.28	2.7262
1	1	P01111_RASN_HUMAN	NRAS	21.22	2.8052
1	1	P10301_RRAS_HUMAN	RRAS	23.47	3.9139
2	2	P62070_RRAS2_HUMAN	RRAS2	23.38	2.9236
1	1	P28482_MK01_HUMAN	MAPK1	41.36	4.5196
1	1	P35222_CTNB1_HUMAN	CTNNB1	85.44	3.1438
1	1	P46940_IQGA1_HUMAN	IQGAP1	189.13	3.4641
1	1	Q15796_SMAD2_HUMAN	SMAD2	52.27	2.3182
5	5	P23458_JAK1_HUMAN	JAK1	133.19	2.172
5	5	P42224_STAT1_HUMAN	STAT1	87.28	2.9462
7	7	P40763_STAT3_HUMAN	STAT3	88.01	3.144
2	2	P68400_CSK21_HUMAN	CSNK2A1	45.11	3.0973
3	3	P67870_CSK2B_HUMAN	CSNK2B	24.93	2.1338
2	2	P48729_KCA1_HUMAN	CSNK1A1	38.91	3.0115
8	8	Q92499_DDX1_HUMAN	DDX1	82.38	3.2822
4	6	O00571_DDX3X_HUMAN	DDX3X	73.2	4.0267
4	4	O15523_DDX3Y_HUMAN	DDX3Y	73.11	3.0997
5	6	P17844_DDX5_HUMAN	DDX5	69.1	2.7447
7	7	P26196_DDX6_HUMAN	DDX6	54.38	3.9909
13	13	Q92841_DDX17_HUMAN	DDX17	80.22	2.9547
6	7	Q9NR30_DDX21_HUMAN	DDX21	87.29	3.1675

1	1	Q9GZR7_DDX24_HUMAN	DDX24	96.27	3.5243
1	1	O00148_DX39A_HUMAN	DDX39A	49.1	2.0665
7	7	Q13838_DX39B_HUMAN	DDX39B	48.96	2.74
3	3	Q7L014_DDX46_HUMAN	DDX46	117.29	2.3912
3	3	Q9H0S4_DDX47_HUMAN	DDX47	50.61	3.4887
1	2	Q9BQ39_DDX50_HUMAN	DDX50	82.51	3.7484
1	1	Q8TDD1_DDX54_HUMAN	DDX54	98.53	3.2442
3	3	O95793_STAU1_HUMAN	STAU1	63.14	2.9951
1	1	Q92900_RENT1_HUMAN	UPF1	124.27	2.2569
2	2	Q13151_ROA0_HUMAN	HNRNPA0	30.82	3.6461
2	2	P09651_ROA1_HUMAN	HNRNPA1	38.72	2.8017
6	7	Q32P51_RA1L2_HUMAN	HNRNPA1L2	34.2	2.7358
7	7	P22626_ROA2_HUMAN	HNRNPA2B1	37.41	3.2476
6	6	P51991_ROA3_HUMAN	HNRNPA3	39.57	3.0494
3	10	Q99729_ROAA_HUMAN	HNRNPAB	36.2	2.8189
1	1	D6RBZ0_D6RBZ0_HUMAN	HNRNPAB	35.66	3.8845
1	1	P07910_HNRPC_HUMAN	HNRNPC	33.65	2.6657
1	1	B7ZW38_HNRC3_HUMAN	HNRNPCL3	32.01	2.9892
1	1	Q14103_HNRPD_HUMAN	HNRNPD	38.41	2.6145
1	1	O14979_HNRDL_HUMAN	HNRNPDL	46.41	2.4245
5	6	P52597_HNRPF_HUMAN	HNRNPF	45.64	3.3512
8	9	P31943_HNRH1_HUMAN	HNRNPH1	49.2	3.1261
3	3	P55795_HNRH2_HUMAN	HNRNPH2	49.23	2.2487
15	21	P61978_HNRPK_HUMAN	HNRNPK	50.94	3.4598
12	13	P52272_HNRPM_HUMAN	HNRNPM	77.46	3.3127
4	4	O43390_HNRPR_HUMAN	HNRNPR	70.9	3.6795
9	11	Q00839_HNRPU_HUMAN	HNRNPU	90.53	3.0678
3	3	Q9BUJ2_HNRL1_HUMAN	HNRNPUL1	95.68	3.1592
1	1	O75643_U520_HUMAN	SNRNP200	244.35	1.8725
2	2	P08621_RU17_HUMAN	SNRNP70	51.53	2.0077
1	1	P09661_RU2A_HUMAN	SNRPA1	28.4	4.6554
2	2	P14678_RSMB_HUMAN	SNRPB	24.59	2.1128
2	3	Q01081_U2AF1_HUMAN	U2AF1	27.85	2.4669
6	6	P26368_U2AF2_HUMAN	U2AF2	53.47	3.1415
3	3	P62987_RL40_HUMAN	UBA52	14.72	3.0926
3	3	P17480_UBF1_HUMAN	UBTF	89.35	2.717

3	5	P62987_RL40_HUMAN	UBA52	14.72	2.911
1	1	P62837_UB2D2_HUMAN	UBE2D2	16.72	3.1967
2	2	P62256_UBE2H_HUMAN	UBE2H	20.64	2.4016
3	3	P63279_UBC9_HUMAN	UBE2I	18	2.6916
3	3	P61086_UBE2K_HUMAN	UBE2K	22.39	3.2048
6	9	P68036_UB2L3_HUMAN	UBE2L3	17.85	3.3187
1	1	O14933_UB2L6_HUMAN	UBE2L6	17.76	4.2125
2	2	P61081_UBC12_HUMAN	UBE2M	20.89	2.4756
3	3	P61088_UBE2N_HUMAN	UBE2N	17.13	3.1043
2	2	Q13404_UB2V1_HUMAN	UBE2V1	16.48	2.5215
1	1	Q15819_UB2V2_HUMAN	UBE2V2	16.35	2.3624

Supplementary Table S5. Summary of pathological categories of patient samples used for primary cell culture and PDX model

Gender	Age	WHO (grade)	Chemotherapy	Radiation	Status
M	63	GBM (IV)	TMZ (11 cycles, 200~350 mg/admin.)	60 Gy, > 30 fract. Doses	Relapsed
M	55	GBM (IV)	N.A	N.A	Primary
F	64	GBM (IV)	N.A	N.A	Primary
M	60	Glioma (III, IV)	N.A	N.A	Primary
F	57	GBM (IV)	N.A	N.A	Primary
F	69	GBM (IV)	N.A	N.A	Primary
M	42	Glioma (II)	N.A	N.A	Primary
M	50	Glioma (III, IV)	N.A	N.A	Primary
M	53	Oligodendrocytoma	N.A	N.A	Metastasis to Dura
F	47	Oligodendrocytoma	N.A	N.A	Primary

Supplementary Table S6. Primer Sequences used for ChIP qPCR Analyses

Gene	Primers	Temp.	GC (%)	Product size
hTuj1-ChIP(A1)-F	CTCGGTTTTCTCTCCGTGCT	60.04	55	214
hTUj1-ChIP(A1)-R	GTCCCATTCACGGCTCATCA	60.11	55	
hTuj1-ChIP(A2)-F	GTCCACTCTGAGATGCCTGG	59.82	60	135
hTUj1-ChIP(A2)-R	CTGGCTGAACACAGACCCTC	60.32	60	
hTuj1-ChIP(A3)-F	CTGCCATTCTGGGAGTAGGC	60.18	60	241
hTUj1-ChIP(A3)-R	GTGGTCTCTTCAGCGAGACG	60.46	60	
hTuj1-ChIP(A5)-F	CTCAGAACTGGGAGCTGCTT	59.68	55	73
hTUj1-ChIP(A5)-R	GGCTTAAGGCTGACTCACCG	60.74	60	
hTuj1-ChIP(B2)-F	CCTGTCCCTTTGTTGGAGGG	60.25	60	220
hTUj1-ChIP(B2)-R	CGAGGTGGGCTAACAATGGA	59.75	55	
hTuj1-ChIP(B3)-F	GCCCCTCCCTCCATTGTTAG	59.82	60	286
hTUj1-ChIP(B3)-R	GATCCCCTGTTCCCCAACAC	60.32	60	
hTuj1-ChIP(B5)-F	AAAGGATCTGCCCTCCGAAC	59.75	55	233
hTUj1-ChIP(B5)-R	GTGGCTGGCCCTGTTGTAAT	60.61	55	
hTuj1-ChIP(C3)-F	TGCCCATCTAGCCACCTCTC	61.05	60	186
hTUj1-ChIP(C3)-R	TCCAGGCCTTAGCACAAAGC	60.61	55	
hTuj1-ChIP(C6)-F	TTTGTGCTAAGGCCTGGATGT	59.92	47.62	70
hTUj1-ChIP(C6)-R	TCGCAGGACCTGTTTTCTCA	59.24	50	
hTuj1-ChIP(C4)-F	TGGGTCTTGAATCCACTCTGC	60	52.38	130
hTUj1-ChIP(C4)-R	GTTCCAGGGAACCCACAACC	60.83	60	
hTuj1-ChIP(C1)-F	TTTACAGGGGCTGGTGGTTG	60.18	55	88
hTUj1-ChIP(C1)-R	CACTTGAGTCGGGGACCTTG	60.32	60	
hLbx1-ChIP(B10)-F	ACCAGGGCAAGTCTTGGCTA	61.13	55	99
hLbx1-ChIP(B10)-R	ACTCTTAGGTAGGGGGCAGA	58.98	55	
hLbx1-ChIP(B9)-F	GTCTCTGCCCCCTACCTAAGA	60.06	57.14	87
hLbx1-ChIP(B9)-R	CCGCAATTAGGGTGTCTCTGT	60.07	52.38	
hLbx1-ChIP(B4)-F	AGCCAGACAGAGACACCCTA	59.59	55	115
hLbx1-ChIP(B4)-R	CGTGGGGAATCGAGAGTCTT	59.18	55	
hLbx1-ChIP(B6)-F	GTCCCCGGCAAAAGACTCTC	60.67	60	110
hLbx1-ChIP(B6)-R	GCTCTTTCCGCAGTCTGCTT	60.95	55	
hLbx1-ChIP(C1)-F	CCTGGGGAGAGGGAATCTGA	60.03	60	248
hLbx1-ChIP(C1)-R	AAGTGAGCAAGATTGCCGGA	59.96	50	
hLbx1-ChIP(C3)-F	CTCCGGCAATCTTGCTCACT	60.39	55	95

hLbx1-ChIP(C3)-R	CCTGGCTACTCTTCAGACGC	60.18	60	
hLbx1-ChIP(C5)-F	ATGGGCGTCTGAAGAGTAGC	59.54	55	227
hLbx1-ChIP(C5)-R	TGCGAGTTCCTGAGAGCAAA	59.61	50	
hLbx1-ChIP(C7)-F	TTGCTCTCAGGAACTCGCAG	60.04	55	75
hLbx1-ChIP(C7)-R	ACAGATCCCGGGCCCTAAG	60.77	63.16	
hLbx1-ChIP(A8)-F	GGCTGTAAGTTGGGAAGCTCA	60.27	52.38	87
hLbx1-ChIP(A8)-R	GGACTGACAGGCGCATTAGG	60.81	60	
hLbx1-ChIP(A6)-F	CTAATGCGCCTGTCAGTCCG	61.15	60	85
hLbx1-ChIP(A6)-R	CGGGTGCAATAAAGGAGCAG	59.27	55	
hLbx1-ChIP(A3)-F	CTGCTCCTTTATTGCACCCG	59.27	55	178
hLbx1-ChIP(A3)-R	GGTTCCCACCACTCTTTCGG	60.61	60	
hDlx1-ChIP(A5)-F	GGCCTTGGGAGATGTTTGCT	60.61	55	372
hDlx1-ChIP(A5)-R	AGGCGTGGACGAGGTATTTT	59.39	50	
hDlx1-ChIP(A1)-F	AATACCTCGTCCACGCCTTC	59.82	55	90
hDlx1-ChIP(A1)-R	AGCCACTCTTGGCTGGAATC	60.03	55	
hDlx1-ChIP(B1)-F	GTGGATGCGTCTTACCCGAG	60.53	60	75
hDlx1-ChIP(B1)-R	GATTGGTCCGAGGCGCT	59.43	64.71	
hDlx1-ChIP(C6)-F	CCCAAAAGGGAAGCAGAGGA	59.59	55	94
hDlx1-ChIP(C6)-R	CGGGGCTGTTGAGACTTTCT	59.96	55	
hDlx1-ChIP(C1)-F	AGAAAGTCTCAACAGCCCCG	59.96	55	112
hDlx1-ChIP(C1)-R	ACAGTGCATGGAGTAGTGCC	60.04	55	
hDlx1-ChIP(C10)-F	TCTCCTTCTCCCATGTCCCA	59.58	55	140
hDlx1-ChIP(C10)-R	CTGCTGACCGAGTTGACGTA	59.76	55	
hGFAP-ChIP(2)-F	CCATTGTGTCCTCTTCTGCCT	60	52.38	359
hGFAP-ChIP(2)-R	CTCTACTCCTCACCCCTCCTG	60.41	61.9	
hGFAP-ChIP(8)-F	TCCAGCGACTCAATCTTCCTCT	60.89	50	138
hGFAP-ChIP(8)-R	TAAGGCAAGGCTGAGGAATGGG	62.35	54.55	

Supplememtary Table S7. Primer Sequences used for Quantitative PCR Analyses

Genes	Primer Sequences	Tm (˚C)	GC Content

DLX1 (F)	TGCCAGAAAGTCTCAACAGCC	57.7	52.4
DLX1 (R)	CGAGTGTAAACAGTGCATGGA	55.2	47.6
DLX2 (F)	ACACCTCCTACGCTCCCTATG	58.1	57.1
DLX2 (R)	TCACTATCCGAATTTCAGGCTCA	55.9	43.5
TUJ1 (F)	GGCCAAGGGTCACTACACG	58.2	63.2
TUJ1 (R)	GCAGTCGCAGTTTTCACACTC	56.8	52.4
NeuroD1 (F)	GTCTCCTTCGTTCAGACGCTT	57	52.4
NeuroD1 (R)	AAAGTCCGAGGATTGAGTTGC	55.3	47.6
GAD67 (F)	GCTTCCGGCTAAGAACGGT	57.6	57.9
GAD67 (R)	TTGCGGACATAGTTGAGGAGT	56	47.6
GFAP (F)	AGGTCCATGTGGAGCTTGAC	57.1	55
GFAP (R)	GCCATTGCCTCATACTGCGT	58.2	55
S100b (F)	TGGCCCTCATCGACGTTTTC	57.8	55
S100b (R)	ATGTTCAAAGAACTCGTGGCA	54.9	42.9
MBP (F)	CCGAGAAGGCCAGTACGAATA	56.2	52.4
MBP (R)	CTGAGGTTGTCCGTGAAAGTT	55.1	47.6
MAG (F)	GGTGTCTGGTACTTCAATAGCC	55.1	50
MAG (R)	CTCTCGTGGACTACTTGGGTG	56.9	57.1

CD24 (F)	CTCCTACCCACGCAGATTTATTC	55.2	47.8
CD24 (R)	AGAGTGAGACCACGAAGAGAC	55.8	52.4
CD44 (F)	CTGCCGCTTTGCAGGTGTA	58.4	57.9
CD44 (R)	CATTGTGGGCAAGGTGCTATT	56	47.6
CD133 (F)	AGTCGGAAACTGGCAGATAGC	57	52.4
CD133 (R)	GGTAGTGTTGTACTGGGCCAAT	57.1	50
CXCR4 (F)	ACGCCACCAACAGTCAGAG	57.5	57.9
CXCR4 (R)	AGTCGGGAATAGTCAGCAGGA	57.5	52.4
OCT4 (F)	GGGAGATTGATAACTGGTGTGTT	54.8	43.5
OCT4 (R)	GTGTATATCCCAGGGTGATCCTC	56.2	52.2
NANOG (F)	TTTGTGGGCCTGAAGAAAACT	55	42.9
NANOG (R)	AGGGCTGTCCTGAATAAGCAG	56.9	52.4
SOX2 (F)	TACAGCATGTCCTACTCGCAG	56.4	52.4
SOX2 (R)	GAGGAAGAGGTAACCACAGGG	56.8	57.1
KLF4 (F)	CGGACATCAACGACGTGAG	55.8	57.9
KLF4 (R)	GACGCCTTCAGCACGAACT	58	57.9
NESTIN (F)	CTGCTACCCTTGAGACACCTG	57.2	57.1
NESTIN (R)	GGGCTCTGATCTCTGCATCTAC	56.8	54.5

PAX6 (F)	TGGGCAGGTATTACGAGACTG	56.3	52.4
PAX6 (R)	ACTCCCGCTTATACTGGGCTA	57.4	52.4
BMI1 (F)	CCACCTGATGTGTGTGCTTTG	56.7	52.4
BMI1 (R)	TTCAGTAGTGGTCTGGTCTTGT	55.4	45.5
MBD3 (F)	CAGCCGGTGACCAAGATTACC	58	57.1
MBD3 (R)	CTCCTCAGCAATGTCGAAGG	55.5	55
GAPDH (F)	CTGGGCTACACTGAGCACC	58	63.2
GAPDH (R)	AAGTGGTCGTTGAGGGCAATG	58	52.4
GAPDH: Glyceraldehyde-3-phosphate dehydrogenase			

Supplememtary Table S8. Source, catalog, and clone informations for commercial antibodies used in this study.

Antibodies	**Company**	**Catalog Number**	**Host Species**
CD133	Life Technologies, Carlsbad, CA	MA5-18323	Mouse
CD44	Novous Biologicals, Littleton, CO	NBP1-31488	Rabbit
CXCR4	Thermo Scientific, Rockford, IL	PA3-305	Rabbit
MBD3	Cell Signaling Technology, Beverly, MA	99169S	Rabbit
α-tubulin	Santa Cruz Biotechnology, Santa Cruz, CA	sc-398103	Mouse
HA (12CA5)	Santa Cruz Biotechnology, Santa Cruz, CA	sc-57592	Mouse
HA (C29F4)	Cell Signaling Technology, Beverly,	3724S	Rabbit

	MA		
Flag	Sigma, St. Louis, MO	SAB4301135	Mouse
Myc-tag	Cell Signaling Technology	2276S	Mouse
β-TrCP	Cell Signaling Technology, Beverly, MA	11984S	Rabbit
phosphoserine (PSR-45)	Abcam Inc., Cambridge, MA	ab6639	Mouse
CK1α	Novous Biologicals, Littleton, CO	NBP1-18880	Rabbit
Nestin	Abcam Inc., Cambridge, MA	ab22035	Mouse
Ki67	Sigma, St. Louis, MO	SAB5600249	Rabbit
IgG	Abcam Inc., Cambridge, MA	ab171870	Rabbit
HDAC1	Cell Signaling	34589S	Rabbit
HDAC2	Cell Signaling	57156S	Rabbit
MTA1	Cell Signaling	5647S	Rabbit
Histone H3 (acetyl K27)	Abcam Inc., Cambridge, MA	ab4729	Rabbit
Histone H3 (acetyl K9 + K14 + K18 + K23 + K27)	Abcam Inc., Cambridge, MA	ab47915	Rabbit
RbAP46 (V415)	Cell Signaling	6882	Rabbit
MBD2	Santa Cruz Biotechnology, Santa Cruz, CA	sc-514062	Mouse
MGMT	Novous Biologicals, Littleton, CO	NBP2-68885	Rabbit
β-Tubulin III	Covance, Princeton, NJ	MMS-435P	Mouse
GFAP	Cell Signaling Technology	12389S	Rabbit
FITC-CD44	Miltenyi Biotec Inc., Auburn, CA	130-113-903	Conjugation
CD44-APC, human (clone: DB105)	Miltenyi Biotec Inc., Auburn, CA	130-113-893	Conjugation
CD133/1 (AC133)-PE, human (clone: AC133)	Miltenyi Biotec Inc., Auburn, CA	130-108-062	Conjugation
PEcy7-CXCR4 (clone: 12G5)	Biolegend, San Diego, CA	306514	Conjugation
anti-rabbit Alexa Fluor 488	Molecular Probes, Eugene, OR	A27034	Secondary
anti-mouse Alexa Fluor 488	Molecular Probes, Eugene, OR	A28175	Secondary
anti-rabbit Alexa Fluor 555	Molecular Probes, Eugene, OR	A27039	Secondary
anti-mouse Alexa Fluor 555	Molecular Probes, Eugene, OR	A28180	Secondary

Data set 1. mRNA expression data of RNA sequencing consisting of GBM patient (*n*=20) and adjacent normal (*n*=19) brain tissues.